

FOR REFERENCE

NOT TO BE TAKEN FROM THIS ROOM

TRANSIENT RESPONSES OF A THICK-WALLED
LAYERED SPHERICAL SHELL BY THE RAY THEORY

by

SENCAN DEREBEYOĞLU

B.S. in M.E., Boğaziçi University, 1980

Bogazici University Library



14

39001100315871

Submitted to the Institute for Graduate Studies in
Science and Engineering in partial fulfillment of
the requirements for the degree of

Master of Science

in

Mechanical Engineering

Boğaziçi University

1983

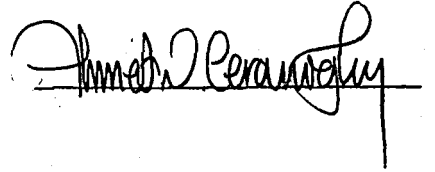


178688

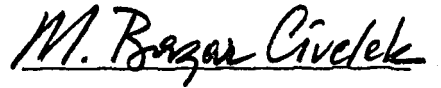
TRANSIENT RESPONSES OF A THICK-WALLED
LAYERED SPHERICAL SHELL BY THE RAY THEORY

APPROVED BY

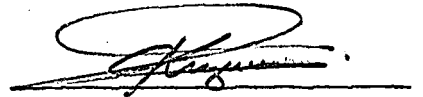
Yard. Doç. Dr. Ahmet N. CERANOĞLU
(Thesis Supervisor)



Doç. Dr. M. Başar CİVELEK



Yard. Doç. Dr. Ahmet KUZUCU



DATE OF APPROVAL: December 30, 1983

TO MY FATHER

ACKNOWLEDGEMENTS

I would like to express my sincere gratitude to my thesis supervisor Yard. Doç. Dr. AHMET N. CERANOĞLU for his valuable advice, guidance, encouragement and for all the help he has given to me throughout this study.

Special appreciation is expressed to Doç. Dr. M. BAŞAR CİVELEK and Yard. Doç. Dr. AHMET KUZUCU for their interest and helpful suggestions. Particular thanks are extended to GÜLSEN KARŞİT for her patience and diligence in typing; and Mech. Eng. FARUK KAMA for his help in drawing the figures of this work.

TRANSIENT RESPONSES OF A THICK-WALLED LAYERED SPHERICAL SHELL BY THE RAY THEORY

ABSTRACT

In this work, the transient response of a thick-walled layered spherical shell subjected to radially symmetric loadings is studied using the ray theory. Normal mode solution in the Fourier transform space is expanded into a series where each term represents a spherical harmonic wave. The inverse transform of these terms which are called ray integrals can be obtained in closed form. Since each ray reaching a receiver point has a unique arrival time, only a finite number of them should be considered once the time interval of interest is specified. Summation of these rays up to a specific time gives the exact solution of the transient response. Since the number of rays to be considered increases geometrically as the time interval increases, the method loses its advantage in calculating the long time responses of the medium. Similar problem will arise in those cases where the shell is a thin one.

A computer program is developed in order to investigate the transient displacements and radial and tangential stresses, and numerical results are given for a suddenly applied uniform

internal pressure case. The peak value for tangential stress is found to be 142 per cent of applied pressure in the two-layered shell, although this value was 165 per cent for a single layered shell having the same material properties with the first layer. The reason for radial stress changes from compression to tension due to dynamic pressure can be found in the result of multiple reflection of waves. As the radial displacement case is investigated, it is found that the peak value of 1.31 unit of displacement is reached for the two-layered shell although it was 1.70 for the single layered case.

İŞIN TEORİSİYLE KALIN KATMANLI KÜRESEL KABUĞUN GEÇİŞ REJİMİNDEKİ DAVRANIŞI

ÖZET

Bu çalışmada, ışın teorisi uygulanarak kalın katmanlı küresel bir kabuğun radyal simetrik yükler altında geçiş rejimindeki davranışı incelenmiştir. Fourier dönüşümü cinsinden elde edilen normal mod çözümü, her terimi küresel harmonik bir dalgayı temsil eden sonsuz bir seri halinde yazılabilir. Her terime bir ışın adı verilmiştir. Bu ışınların ters dönüşümü kapalı olarak bulunabilir. Gözlenen bir noktaya gelen her ışının ayrı ve tek varış zamanı olacağından, gözlem süresi belirlendikten sonra sadece sonlu sayıda ışının incelenmesi gerekmektedir. Belli bir süre içerisinde gelen tüm ışınların toplamı ortamın geçiş rejimi içindeki davranışını kesin olarak verir. Süre uzadıkça ışın sayısı geometrik olarak artacağından, uzun süreli davranışın hesaplanmasında metod avantajını kaybeder. Kabuğun ince olması hallerinde de aynı problem ortaya çıkacaktır.

Geçiş rejimi içindeki deplasmanları, radyal ve teğetsel gerilmeleri bulmak için bir bilgisayar programı geliştirilmiş ve aniden uygulanan düzgün iç basınç için bulunan sayısal sonuçlar sunulmuştur. İki katmanlı küresel kabukta en yüksek teğetsel

gerilme deęeri uygulanan basıncın yüzde 142 si olarak bulunmuştur. Birinci katmanla aynı malzeme özelliklerine sahip tek katlı küresel kabukta ise bu deęer yüzde 165 olarak elde edilmişti. Dinamik yüklemde radyal gerilmenin sıkıştırmadan çekmeye dönmesinin sebebi olarak ışınların karşılıklı yansımaları gösterilebilir. Radyal deplasman durumu incelendiğinde ise en yüksek deęer 1.31 birim olarak bulunmuşken, bunun tek katmanlı küresel kabukta 1.70 birim olduęu gözlenmiştir.

TABLE OF CONTENTS

	Page
ACKNOWLEDGEMENTS	iv
ABSTRACT	v
ÖZET	vii
LIST OF FIGURES	x
LIST OF TABLES	xii
LIST OF SYMBOLS	xiii
I. INTRODUCTION	1
II. EQUATIONS OF MOTION	5
A. General Formulation	5
B. Layered Spherical Shell	8
III. NORMAL MODE SOLUTION OF THE PROBLEM	12
IV. RAY THEORY APPLICATION	17
A. Introduction	17
B. The Coefficients of Reflection and Transmission	18
C. Ray Theory Solution	24
V. TRANSIENT SOLUTION FOR AN INTERNAL PRESSURE	31
A. Problem and Initial Rays	31
B. Higher Order Rays	34
VI. NUMERICAL RESULTS AND DISCUSSION	41
VII. CONCLUSIONS	51
APPENDIX A	53
APPENDIX B	55
BIBLIOGRAPHY	57
REFERENCES NOT CITED	59

LIST OF FIGURES

	Page	
FIGURE 2.1	Dynamic loadings and a typical volume element of a thick-walled spherical shell	5
FIGURE 2.2	Layered spherical shell	9
FIGURE 4.1	Initial outgoing wave in the first shell	19
FIGURE 4.2	Initial reflected and transmitted waves due to internal pressure	20
FIGURE 4.3	Converging wave after reflected at $r=1$.	21
FIGURE 4.4	Initial rays in the second layer	29
FIGURE 5.1	Path of integration for $\bar{\phi}_{oo}^{(1)}(r, \alpha)$	32
FIGURE 5.2	Paths of the fundamental rays	33
FIGURE 6.1	Values of individual rays at the inner surface ($r=1$., $\ell=2$., and $b=3$.)	44
FIGURE 6.2	Variation of tangential stress with r in a two-layered shell for locations in the first layer ($\ell=2$., $b=3$.)	45
FIGURE 6.3	Variation of tangential stress with r in a two-layered shell for locations in the second layer ($\ell=2$., $b=3$.)	46
FIGURE 6.4	Variation of radial stress in a two-layered shell for various locations in the first layer ($\ell=2$., $b=3$.)	47
FIGURE 6.5	Variation of radial stress in a two-layered shell for various locations in the second layer ($\ell=2$., $b=3$.)	48
FIGURE 6.6	Radial displacement in a two-layered shell at various locations in the first layer ($\ell=2$., $b=3$.)	49

FIGURE 6.7

Radial displacement in a two-layered shell
at various locations in the second layer
($l=2.$, $b=3.$)

50

LIST OF TABLES

	Page
TABLE 4.1 Reflection and transmission coefficients	23
TABLE 6.1 Material properties of the layers for the sample problem.	41

LIST OF SYMBOLS

a	inner radius of the spherical shell
b	outer radius of the spherical shell
c_i	dilatational wave speed of the i -th-shell = $\sqrt{(\lambda_i + 2\mu_i)/\rho_i}$
c_{ijk}	a constant = $\alpha\beta_i k h_0^{(j)}(\beta_i k \alpha) + 4\kappa_i h_0^{(j)'}(\beta_i k \alpha)$
d_{ijk}	a constant = $\alpha\beta_i h_0^{(j)'}(\beta_i k \alpha)$
$h_0^{(1),(2)}(z)$	zeroth-order spherical Hankel functions of the first and second kinds, respectively = $\exp(\pm iz)/(\pm iz)$
$h_0'(z)$	derivative of the zeroth-order spherical Hankel function wrt $z = dh_0(z)/dz$
m_i	a constant = $2\kappa_i(\kappa_i^{-1} - 1)^{1/2}$
n_i	a constant = $2\kappa_i$
$p_{1,2}(t)$	inner, outer pressure loading
r	radial distance
$R_{ij}(\alpha)$	reflection coefficient for a spherical harmonic wave which is reflected at the interface $r=j$, and turns back to the i -th shell
$T_{ij}(\alpha)$	transmission coefficient of the spherical harmonic wave travelling from i -th shell to the j -th shell.
t	time
u_r	radial displacement
y	a constant = $4(\kappa_1 - \kappa_2 \eta_2)$
α	frequency
β_i	dilatational wave speed ratio = c_1/c_i
γ_j	a constant = $m_j + in_j$

γ_j^*	a constant = $m_j - in_j$
$\epsilon_r, \epsilon_\theta, \epsilon_\phi$	strain components
n_i	a constant = $\rho_i c_i^2 / \rho_1 c_1^2$
κ_i	a constant = $(1-2\nu_i)/(2-2\nu_i) = \mu_i/(\lambda_i+2\mu_i)$
λ_i, μ_i	Lamé constants for i-th shell
ν_i	Poisson's ratio for i-th shell
ρ_i	mass density of the i-th shell
$\sigma_r, \sigma_\theta, \sigma_\phi$	normal stress components
$\Phi^{(i)}(r, t)$	displacement potential for i-th shell
$\phi_{jk}^{(i)}(r, t)$	waves generated by the inner pressure coming to the point in the i-th shell, j showing ray index and k stands for the direction (outgoing, 0, or incoming, 1)
$\Psi_{jk}^{(i)}(r, t)$	waves generated by the outer pressure
$\bar{\chi}(r, \alpha)$	an arbitrary variable = $r \bar{\Phi}^{(i)}(r, \alpha)$
ω	angular frequency
ℓ	radius of the interface

I. INTRODUCTION

Realizing the effects of internal explosion or impact on a spherical shell, an analysis of the transient response of the shell under such dynamic loading is necessary. This work is aimed to such an analysis of a thick-walled layered elastic spherical shell, subject to radially symmetric loadings.

Even though Lamé considered the static problem in 1852(1)*, the dynamic problem received attention only after 1955 (2). In general three different methods of solution exist,

1. The Normal Mode Analysis,
2. The Method of Characteristics,
3. The Ray Theory.

The first method was used by Baker and Allen (3) where they studied the dynamic response of an elastic spherical shell subject to a spherically symmetric, internally applied pressure pulse. Their solution is in the form of an infinite series, each term of which is the normal mode of the shell.

Baker (4) has also studied the character and frequencies of the normal-mode vibration of a thin spherical shell and has shown by experiment that such modes physically do exist. Later, Cinelli (5) using the finite Hankel transform arrived at the same solution. However, the main difficulty with the normal mode analy-

* Parenthetical references refer to the bibliography.

sis is the slow convergence of the series especially for large thicknesses of the shell.

As an alternative, Rose, et al (6) applied the method of characteristics to the same problem. The method was first presented by Chou and Koenig (7) in their analysis of elastic waves with either cylindrical or spherical symmetry. In this method, the continuous domain is replaced by discrete points and the properties at each grid point is calculated. A numerical procedure involving stepwise integration along the characteristics is employed to solve the problem for various inputs. The accuracy of the solution depends on the mesh size used for the numerical integration.

Later, Pao and Ceranoğlu (8) presented the analysis using the Ray Theory. They have formulated the general solution for transient waves in a thick-walled spherical shell generated by uniformly applied pressures at the inner and outer surfaces. In this work, we will extend their method to study the propagation of waves in a layered spherical shell.

Method of the Ray Theory takes its name from the geometric theory of light by following the propagation of a pulse along a ray-path. In the theory of geometrical optics a light ray is defined to be the orthogonal trajectories to the wave fronts. The intensity of light along a ray-path may be determined from the asymptotic solution of wave equation at high frequencies (9). This is known as the Ray Theory of optics.

The general solution for waves in a bounded medium can be sorted out into different rays by using the Bromwich expansion or the like. Each term in such an expansion represents waves traveling along a given ray-path. In the literature, this approach is also known as the ray theory, but it is different from the ray theory of geometrical optics. Van der Pol and Bremmer (10) developed such a ray theory to calculate the diffraction of radio waves by the earth. Pao and Gajewski (11) present a review article concerning the method as applied to elastic waves travelling in horizontally layered medium.

In the ray theory, it is assumed that waves propagate along different ray-paths formed by reflections and transmissions taking place at the interfaces of the shell. The Fourier transformed solution of the equations of motion can be sorted out into an infinite series when each term represents such rays. Inverse Fourier transform of these terms are called ray integrals. These integrals can either be integrated analytically in closed form as for the axisymmetric loadings of spherical shell, or evaluated numerically for nonsymmetric loadings. Since the rays arrive at a point of observation in successive order according to the theory, the transient solution obtained by summing up these rays is exact up to the arrival time of the next ray. The method is most effective for early time solutions of thick-walled shells, since the number of rays to be considered increases as the duration of observation lengthens or the thickness of the shell decreases. In such cases, normal mode solution is more economical.

In the following chapter, we will present the general equations of motion for an elastic thick-walled spherical shell and their extensions to waves in layered spherical shells. The normal mode solution of the problem will be given in Chapter III, while Chapter IV illustrates the application of the ray theory to the problem. The solution due to a suddenly applied internal pressure will then be presented in Chapter V, with Chapter VI devoted to numerical results and discussion.

II. EQUATIONS OF MOTION

A. GENERAL FORMULATION

Considering a typical volume element, a spherical square (Figure 2.1.a) with radial thickness, dr ; it can be shown that the response of an isotropic, homogeneous, elastic spherical shell, subject to radially symmetric loadings (Figure 2.1.b), is governed by the equation (12):

$$\frac{\partial \sigma_r}{\partial r} + \frac{2}{r} (\sigma_r - \sigma_\theta) = \rho \frac{\partial^2 u_r}{\partial t^2} \quad (2.1)$$

where

σ_r, σ_θ - radial and tangential stress components.

r - radial distance

u_r - radial displacement

ρ - mass density

t - time

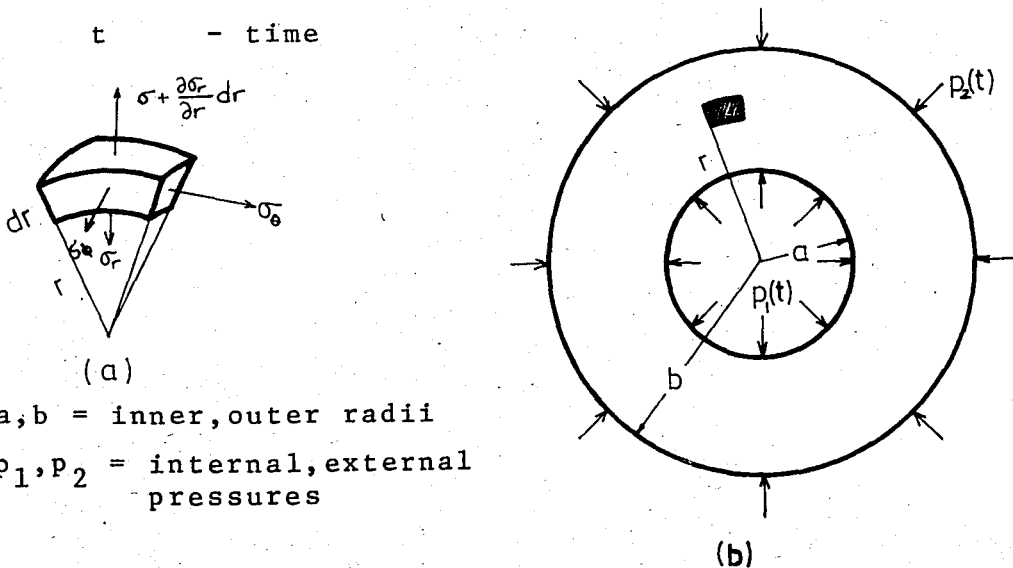


FIGURE 2.1. Dynamic loadings and a typical volume element of a thick-walled spherical shell.

For spherically symmetric loadings, all shear strains and stresses are zero and the displacement is a purely radial one, i.e.,

$$u_r = u_r(r, t), \quad u_\theta = 0, \quad u_\phi = 0 \quad (2.2)$$

The strain-displacement relations in spherical coordinates are
(12)

$$\epsilon_r = \frac{\partial u_r}{\partial r}, \quad \epsilon_\theta = \epsilon_\phi = \frac{u_r}{r} \quad (2.3)$$

where ϵ_r , ϵ_θ , ϵ_ϕ are the normal strain components.

Using the above expressions in the Hooke's law, one can show that the stresses are related only to the radial component of the displacement through the relations

$$\sigma_r = (\lambda + 2\mu) \frac{\partial u_r}{\partial r} + 2\lambda \frac{u_r}{r} \quad (2.4)$$

$$\sigma_\theta = \sigma_\phi = \lambda \frac{\partial u_r}{\partial r} + 2(\lambda + \mu) \frac{u_r}{r} \quad (2.5)$$

where λ and μ are the Lamé constants. Substituting the above expressions into Eq (2.1), we get

$$\frac{\partial^2 u_r}{\partial r^2} + \frac{2}{r} \frac{\partial u_r}{\partial r} - \frac{2}{r^2} u_r = \frac{1}{c^2} \frac{\partial^2 u_r}{\partial t^2} \quad (2.6)$$

where $c = \sqrt{(\lambda+2\mu)/\rho}$ is the velocity of the pressure waves travelling inside the medium.

If the shell is subjected to internal and external pressures, the required boundary conditions are

$$\sigma_r(a,t) = -p_1(t)$$

$$\sigma_r(b,t) = -p_2(t) \quad (2.7)$$

and in the case where the medium is initially at rest the initial conditions pertinent to Eq (2.6) are

$$u_r(r,0) = \frac{\partial u_r(r,0)}{\partial t} = 0 \quad (2.8)$$

The solution of Eq (2.6) is simplified to a great extent by introducing the displacement potential Φ , where

$$u_r(r,t) = \frac{\partial \Phi}{\partial r} \quad (2.9)$$

Thus, Eq (2.6) takes the form

$$\frac{\partial}{\partial r} \left(\frac{\partial^2 \Phi}{\partial r^2} + \frac{2}{r} \frac{\partial \Phi}{\partial r} - \frac{1}{c^2} \frac{\partial^2 \Phi}{\partial t^2} \right) = 0 \quad (2.10)$$

Integrating the above equation with respect to r , we get

$$\frac{\partial^2 \Phi}{\partial r^2} + \frac{2}{r} \frac{\partial \Phi}{\partial r} - \frac{1}{c^2} \frac{\partial^2 \Phi}{\partial t^2} = F(t) \quad (2.11)$$

where $F(t)$ is an arbitrary function of time only. Note that the particular solution of Eq (2.11) will also be a function of time

only, say $\phi_p(t)$. However, such a solution will not contribute to the displacement, u_r , as seen from Eq(2.9), hence, it will not contribute to the stresses either. Thus, we can set $F(t) \equiv 0$ with no loss of generality and obtain

$$\frac{\partial^2 \phi}{\partial r^2} + \frac{2}{r} \frac{\partial \phi}{\partial r} = \frac{1}{c^2} \frac{\partial^2 \phi}{\partial t^2} \quad (2.12)$$

as the equation of motion.

The components of the stress tensor in terms of the potential ϕ are

$$\sigma_r(r, t) = \rho \frac{\partial^2 \phi}{\partial t^2} - \frac{4\mu}{r} \frac{\partial \phi}{\partial r} \quad (2.13)$$

$$\sigma_\theta(r, t) = (1 - 2\kappa)\rho \frac{\partial^2 \phi}{\partial t^2} + \frac{2\mu}{r} \frac{\partial \phi}{\partial r} \quad (2.14)$$

where $\kappa = \mu/(\lambda + 2\mu) = (1-2\nu)/(2-2\nu)$, ν is the Poisson's ratio.

Formulation of the problem outlined in this section will be modified for the case of a layered shell in the following section.

B. LAYERED SPHERICAL SHELL

We will now consider a layered spherical shell with two layers of different materials (Figure 2.2), subject to both internal and external pressures. Subscripts and superscripts 1 and 2 will be used to identify those quantities related to the inner

and outer layers respectively. With this notation Eq (2.12) can be written as

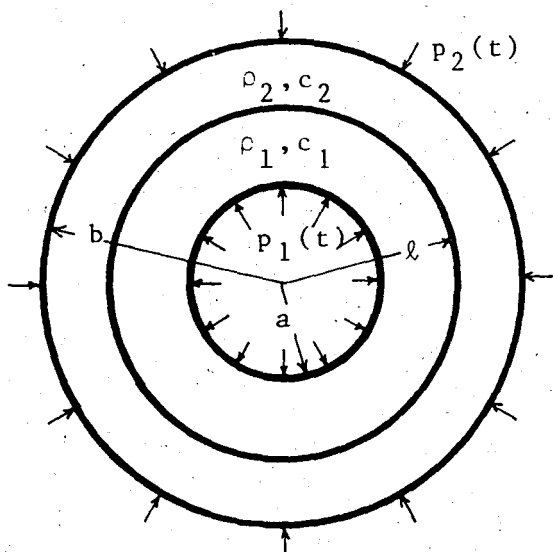
$$\frac{\partial^2 \phi^{(i)}}{\partial r^2} + \frac{2}{r} \frac{\partial \phi^{(i)}}{\partial r} = \frac{1}{c_i^2} \frac{\partial^2 \phi^{(i)}}{\partial t^2} \quad i=1,2 \quad (2.15)$$

where it is understood that

$$u_r^{(i)} = \frac{\partial \phi^{(i)}}{\partial r} \quad (2.16)$$

The Boundary conditions pertinent to the problem are then

$$\begin{aligned} \sigma_r^{(1)}(a,t) &= -p_1(t) & \sigma_r^{(2)}(b,t) &= -p_2(t) \\ \sigma_r^{(1)}(\ell,t) &= \sigma_r^{(2)}(\ell,t) & u_r^{(1)}(\ell,t) &= u_r^{(2)}(\ell,t) \end{aligned} \quad (2.17)$$



- $\rho_{1,2}$ - mass density
- $c_{1,2}$ - dilatational wave speeds
- ℓ - radius of the interface

FIGURE 2.2. Layered Spherical Shell.

whereas the initial conditions are

$$\dot{\Phi}^{(i)}(r,0) = \frac{\partial \Phi^{(i)}(r,0)}{\partial t} = 0 \quad (2.18)$$

$i=1,2$

and the stress components are given by

$$\sigma_r^{(i)}(r,t) = \rho_i \frac{\partial^2 \Phi^{(i)}}{\partial t^2} - \frac{4\mu_i}{r} \frac{\partial \Phi^{(i)}}{\partial r} \quad (2.19)$$

$$\sigma_\theta^{(i)}(r,t) = (1-2\kappa_i) \rho_i \frac{\partial^2 \Phi^{(i)}}{\partial t^2} + \frac{2\mu_i}{r} \frac{\partial \Phi^{(i)}}{\partial r}$$

$i=1,2$

where $\kappa_i = \mu_i / (\lambda_i + 2\mu_i) = (1-2\nu_i) / (2-2\nu_i)$.

Since it is easier to work with non-dimensional quantities, we will introduce the following non-dimensional quantities (denoted by a bar below the variable).

$$\bar{\Phi}^{(i)} = \Phi^{(i)} / a^2 \quad \bar{r} = r/a$$

$$\bar{b} = b/a \quad \bar{\ell} = \ell/a \quad \bar{a} = 1 \quad (2.20)$$

$$\bar{t} = c_1 t/a \quad \bar{u}_r^{(i)} = u_r^{(i)} / a$$

$$\bar{\sigma}^{(i)} = \sigma^{(i)} / \rho_1 c_1^2 \quad \bar{p}_i = p_i / \rho_1 c_1^2$$

Thus, the equations of motion in terms of the non-dimensional variables takes the form

$$\frac{\partial^2 \underline{\phi}^{(i)}}{\partial \underline{r}^2} + \frac{2}{\underline{r}} \frac{\partial \underline{\phi}^{(i)}}{\partial \underline{r}} = \beta_i^2 \frac{\partial^2 \underline{\phi}^{(i)}}{\partial \underline{t}^2} \quad i=1,2 \quad (2.21)$$

where

$$\beta_i = \frac{c_1}{c_i} \quad i=1,2 \quad (2.22)$$

The relation given in Eq (2.19) becomes

$$\begin{aligned} \underline{\sigma}_r^{(i)}(r,t) &= \eta_i \left[\beta_i^2 \frac{\partial^2 \underline{\phi}^{(i)}}{\partial \underline{t}^2} - \left(\frac{4\kappa_i}{\underline{r}} \right) \frac{\partial \underline{\phi}^{(i)}}{\partial \underline{r}} \right] \\ \underline{\sigma}_\theta^{(i)}(r,t) &= \eta_i \left[(1-2\kappa_i) \beta_i^2 \frac{\partial^2 \underline{\phi}^{(i)}}{\partial \underline{t}^2} + \left(\frac{2\kappa_i}{\underline{r}} \right) \frac{\partial \underline{\phi}^{(i)}}{\partial \underline{r}} \right] \end{aligned} \quad (2.23)$$

$i=1,2$

where

$$\eta_i = \frac{\rho_i}{\rho_1 \beta_i^2} \quad i=1,2 \quad (2.24)$$

To simplify the writing of the equations, bars indicating the non-dimensional variables will be dropped with the understanding that all the quantities that we will be working with are in the non-dimensional form.

The solution of Eq (2.21) in the form of normal modes will be presented in the following chapter.

III. NORMAL MODE SOLUTION OF THE PROBLEM

The solution in the form of normal modes will be obtained by first transforming the equations of motion using the complex Fourier transform on time and then solving the resulting transformed equations.

The complex Fourier transform pair of a function $g(r,t)$ is defined as (14),

$$\bar{g}(r,\alpha) = \int_0^{\infty} g(r,t) e^{i\alpha t} dt \quad (3.1.a)$$

$$g(r,t) = \frac{1}{2\pi} \int_{i\epsilon-\infty}^{i\epsilon+\infty} \bar{g}(r,\alpha) e^{-i\alpha t} d\alpha \quad (3.1.b)$$

where ϵ is chosen such that the singularities of $\bar{g}(r,\alpha)$ lie all below the line of integration. α appearing in the above relations can be viewed as both a non-dimensional frequency $\alpha = \omega a/c_1$, where ω is the angular frequency or as the non-dimensional wave number in the radial direction.

Transforming the equations of motion given in Eq (2.21) according to Eq (3.1.a) and solving the resulting equations we get

$$\bar{\phi}^{(i)}(r,\alpha) = A_i h_o^{(1)}(\beta_i r \alpha) + B_i h_o^{(2)}(\beta_i r \alpha) \quad (3.2)$$

$i=1,2$

where

$$h_0^{(1),(2)}(z) = \exp(\pm iz)/(\pm iz) \quad (3.3)$$

are the zeroth-order spherical Hankel functions of the first and second kinds respectively. Details of the solution given by Eq (3.2) are shown in Appendix A.

The constants A_i and B_i are to be determined from the boundary conditions given by Eq (2.17). The transformed form of the boundary conditions are

$$\begin{aligned} \bar{\sigma}_r^{(1)}(1, \alpha) &= -\bar{p}_1(\alpha) & \bar{\sigma}_r^{(2)}(b, \alpha) &= -\bar{p}_2(\alpha) \\ \bar{\sigma}_r^{(1)}(\ell, \alpha) &= \bar{\sigma}_r^{(2)}(\ell, \alpha) & \bar{u}_r^{(1)}(\ell, \alpha) &= \bar{u}_r^{(2)}(\ell, \alpha) \end{aligned} \quad (3.4)$$

The transformed form of the relations between the stresses and the displacement potential are

$$\begin{aligned} \bar{\sigma}_r^{(i)}(r, \alpha) &= \eta_i \left[-\beta_i^2 \alpha^2 \bar{\Phi}^{(i)} - \left(\frac{4\kappa_i}{r} \right) \frac{d\bar{\Phi}^{(i)}}{dr} \right] \\ \bar{\sigma}_\theta^{(i)}(r, \alpha) &= \eta_i \left[-(1-2\kappa_i) \beta_i^2 \alpha^2 \bar{\Phi}^{(i)} + \left(\frac{2\kappa_i}{r} \right) \frac{d\bar{\Phi}^{(i)}}{dr} \right] \end{aligned} \quad (3.5)$$

$i=1, 2$

Applying the boundary conditions to the solution, Eq (3.2),

we get

$$\begin{aligned}
A_1 \alpha c_{111} + B_1 \alpha c_{121} &= \bar{p}_1(\alpha) \\
A_2 \alpha \beta_2 \eta_2 c_{21b} + B_2 \alpha \beta_2 \eta_2 c_{22b} &= \bar{p}_2(\alpha) b \\
A_1 d_{11\ell} + B_1 d_{12\ell} &= A_2 d_{21\ell} + B_2 d_{22\ell} \\
A_1 c_{11\ell} + B_1 c_{12\ell} &= A_2 \beta_2 \eta_2 c_{21\ell} + B_2 \beta_2 \eta_2 c_{22\ell}
\end{aligned} \tag{3.6}$$

where

$$\begin{aligned}
c_{ijk} &= \alpha \beta_i k h_o^{(j)}(\alpha \beta_i k) + 4 \kappa_i h_o^{(j)'}(\alpha \beta_i k) \\
d_{ijk} &= \alpha \beta_i h_o^{(j)'}(\alpha \beta_i k) \\
h_o^{(j)'}(z) &\equiv dh_o^{(j)}(z)/dz
\end{aligned} \tag{3.7}$$

In the above expressions, i denotes the layer, j denotes the order of the spherical Hankel functions, while k takes the values of 1, ℓ , or b for inner, interface and outer radii.

Writing the equations given by Eq (3.6) in matrix form simplifies the work in determining the unknown constants A_i , B_i . Thus, we can write

$$\begin{bmatrix}
c_{111} & c_{121} & 0 & 0 \\
0 & 0 & c_{21b} & c_{22b} \\
d_{11\ell} & d_{12\ell} & -d_{21\ell} & -d_{22\ell} \\
c_{11\ell} & c_{12\ell} & -\beta_2 \eta_2 c_{21\ell} & -\beta_2 \eta_2 c_{22\ell}
\end{bmatrix}
\begin{bmatrix}
A_1 \\
B_1 \\
A_2 \\
B_2
\end{bmatrix}
=
\begin{bmatrix}
\frac{\bar{p}_1(\alpha)}{\alpha} \\
\frac{\bar{p}_2(\alpha) b}{\alpha \beta_2 \eta_2} \\
0 \\
0
\end{bmatrix} \tag{3.8}$$

Using the Cramer's rule A_1 , B_1 , A_2 and B_2 can be written as

$$A_1 = \frac{1}{\Delta_M} \begin{vmatrix} \frac{\bar{p}_1(\alpha)}{\alpha} & c_{121} & 0 & 0 \\ \frac{\bar{p}_2(\alpha)b}{\alpha\beta_2\eta_2} & 0 & c_{21b} & c_{22b} \\ 0 & d_{12\ell} & -d_{21\ell} & -d_{22\ell} \\ 0 & c_{12\ell} & -\beta_2\eta_2c_{21\ell} & -\beta_2\eta_2c_{22\ell} \end{vmatrix} \quad (3.9)$$

where

$$\Delta_M = \begin{vmatrix} c_{111} & c_{121} & 0 & 0 \\ 0 & 0 & c_{21b} & c_{22b} \\ d_{11\ell} & d_{12\ell} & -d_{21\ell} & -d_{22\ell} \\ c_{11\ell} & c_{12\ell} & -\beta_2\eta_2c_{21\ell} & -\beta_2\eta_2c_{22\ell} \end{vmatrix} \quad (3.10)$$

and

$$B_1 = \frac{1}{\Delta_M} \begin{vmatrix} c_{111} & \frac{\bar{p}_1(\alpha)}{\alpha} & 0 & 0 \\ 0 & \frac{\bar{p}_2(\alpha)b}{\alpha\beta_2\eta_2} & c_{21b} & c_{22b} \\ d_{11\ell} & 0 & -d_{21\ell} & -d_{22\ell} \\ c_{11\ell} & 0 & -\beta_2\eta_2c_{21\ell} & -\beta_2\eta_2c_{22\ell} \end{vmatrix} \quad (3.11)$$

$$A_2 = \frac{1}{\Delta_M} \left| \begin{array}{cccc} c_{111} & c_{121} & \frac{\bar{p}_1(\alpha)}{\alpha} & 0 \\ 0 & 0 & \frac{\bar{p}_2(\alpha)b}{\alpha\beta_2\eta_2} & c_{22b} \\ d_{11\ell} & d_{12\ell} & 0 & -d_{22\ell} \\ c_{11\ell} & c_{12\ell} & 0 & -\beta_2\eta_2c_{22\ell} \end{array} \right| \quad (3.12)$$

$$B_2 = \frac{1}{\Delta_M} \left| \begin{array}{cccc} c_{111} & c_{121} & 0 & \frac{\bar{p}_1(\alpha)}{\alpha} \\ 0 & 0 & c_{21b} & \frac{\bar{p}_2(\alpha)b}{\alpha\beta_2\eta_2} \\ d_{11\ell} & d_{12\ell} & -d_{21\ell} & 0 \\ c_{11\ell} & c_{12\ell} & -\beta_2\eta_2c_{21\ell} & 0 \end{array} \right| \quad (3.13)$$

The inverse transform of $\bar{\phi}^{(1)}$ and $\bar{\phi}^{(2)}$ are determined from Eq (3.1.b) where the integrals are evaluated by the residue theorem. The integrand has an infinite number of simple poles at $\Delta_M = 0$ which are all real. Each pole corresponds to a natural frequency of the layered shell. The resulting infinite series solution is a slow converging one for small values of time. We will obtain the solution in terms of rays travelling along different paths inside the medium, in the next chapter, which is more effective for small values of time.

IV. RAY THEORY APPLICATION

A. INTRODUCTION

In this section, we will derive the solution for the transient response of a layered spherical shell subjected to both internal and external pressures, in the form of rays or waves travelling along different paths. Each ray reaching a receiver point has a different and unique arrival time, thus, only a finite number of them should be considered once the time interval of interest is specified. Since the number of rays to be considered increases geometrically as the time interval increases, the method loses its advantage in calculating the long time responses of the medium. Similar problem will arise in those cases where the shell under consideration is a thin one.

Waves traveling inside the medium can be regarded in two groups, (1) those travelling outwards called outgoing waves, and (2) those travelling inwards, called incoming waves. These can be seen from the solution given by Eq (3.2) which has an inverse Fourier transform of the form

$$\begin{aligned} \phi^{(j)}(r, t) = & \frac{1}{2\pi} \int_{i\epsilon-\infty}^{i\epsilon+\infty} A_j(\alpha) h_o^{(1)}(\beta_j r \alpha) e^{-i\alpha t} d\alpha \\ & + \frac{1}{2\pi} \int_{i\epsilon-\infty}^{i\epsilon+\infty} B_j(\alpha) h_o^{(2)}(\beta_j r \alpha) e^{-i\alpha t} d\alpha \quad j=1,2 \end{aligned} \quad (4.1)$$

Noting the definition of $h_o^{(1)}$, the integrand of the first integral is of the form

$$A_j(\alpha) h_o^{(1)}(\beta_j r \alpha) e^{-i\alpha t} = \frac{A_j(\alpha)}{i\beta_j r \alpha} e^{-i\alpha(t - \beta_j r)} \quad (4.2)$$

$j=1,2$

which represents harmonic waves travelling outwards. Similarly the integrand of the second integral

$$B_j(\alpha) h_o^{(2)}(\beta_j r \alpha) e^{-i\alpha t} = \frac{B_j(\alpha)}{-i\beta_j r \alpha} e^{-i\alpha(t + \beta_j r)} \quad (4.3)$$

represents harmonic waves travelling inwards.

Using this notation we will now derive the coefficients of reflection and transmission, in the following section.

B. THE COEFFICIENTS OF REFLECTION AND TRANSMISSION

Let us consider the case where pressure is applied to the internal surface. The wave travelling inside the first layer of the shell prior to any reflections (Figure 4.1) has the form

$$\bar{\phi}_{oo}^{(1)}(r, \alpha) = A_1 h_o^{(1)}(r\alpha) \quad (4.4)$$

where superscript of the wave shows the layer of the receiver point, first subscript stands for the ray index, and the direction of the wave (outgoing, 0, or incoming, 1) is denoted by the second subscript. A_1 is to be determined from the boundary condition

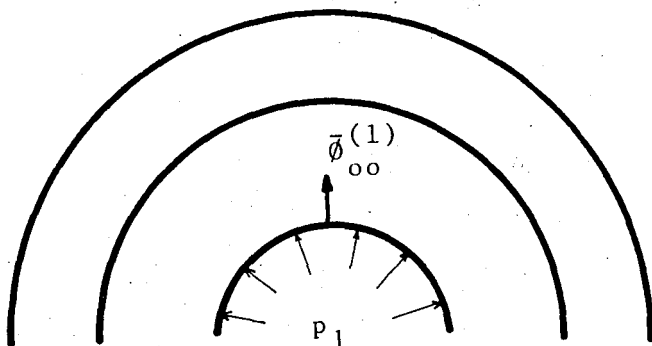


FIGURE 4.1. Initial outgoing wave in the first shell.

$$\bar{\phi}_{r_{oo}}^{(1)}(1, \alpha) = -\bar{p}_1(\alpha) \quad (4.5)$$

Thus,

$$\bar{\phi}_{oo}^{(1)}(r, \alpha) = \frac{\bar{p}_1(\alpha)}{\alpha c_{111}} h_o^{(1)}(r\alpha) \quad (4.6)$$

where c_{111} was defined in Eq (3.7). Inverse Fourier transform of $\bar{\phi}_{oo}^{(1)}$ represents the outgoing wave travelling inside an infinite medium due to a pressurized cavity.

When this wave reaches the intermediate surface at $r=\ell$, it will give rise to two new waves, one reflected back into the first medium, an incoming wave, while the other a transmitted wave travelling outwards in the second medium (Figure 4.2). Displacement potentials representing these waves can be written as

$$\bar{\phi}_{11}^{(1)}(r, \alpha) = \frac{\bar{p}_1(\alpha)}{\alpha c_{111}} R_{1\ell}(\alpha) h_o^{(2)}(r\alpha) \quad (4.7)$$

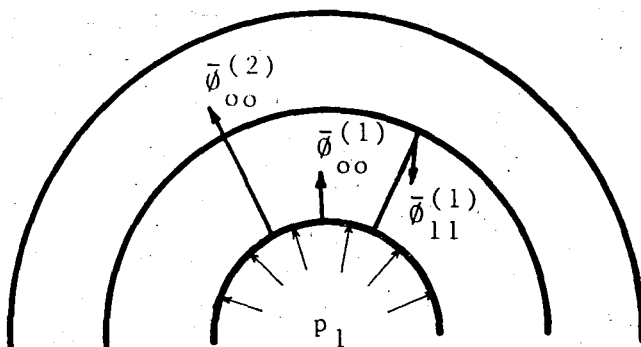


FIGURE 4.2. Initial reflected and transmitted waves due to internal pressure.

$$\bar{\phi}_{oo}^{(2)}(r, \alpha) = \frac{\bar{p}_1(\alpha)}{\alpha c_{111}} T_{12}(\alpha) h_o^{(1)}(\beta_2 r \alpha) \quad (4.8)$$

where $R_{1\ell}$ and T_{12} are called the reflection and transmission coefficients, respectively, for those waves impinging on the interface by travelling inside the first layer. Both of these coefficients are to be determined by making use of the boundary conditions.

$$\bar{u}_{r_{oo}}^{(1)}(\ell, \alpha) + \bar{u}_{r_{11}}^{(1)}(\ell, \alpha) = \bar{u}_{r_{oo}}^{(2)}(\ell, \alpha) \quad (4.9)$$

$$\bar{\sigma}_{r_{oo}}^{(1)}(\ell, \alpha) + \bar{\sigma}_{r_{11}}^{(1)}(\ell, \alpha) = \bar{\sigma}_{r_{oo}}^{(2)}(\ell, \alpha) \quad (4.10)$$

Going through the analysis, we get

$$R_{1\ell}(\alpha) = \frac{c_{11\ell} d_{21\ell} - \beta_2 \eta_2 c_{21\ell} d_{11\ell}}{\beta_2 \eta_2 c_{21\ell} d_{12\ell} - c_{12\ell} d_{21\ell}} \quad (4.11)$$

$$T_{12}(\alpha) = \frac{c_{11\ell}^d d_{12\ell} - c_{12\ell}^d d_{11\ell}}{\beta_2 \eta_2 c_{21\ell}^d d_{12\ell} - c_{12\ell}^d d_{21\ell}} \quad (4.12)$$

We also have to introduce the reflection coefficient, $R_{11}(\alpha)$, for the waves caused by the reflection of the waves impinging on the inner surface, (Figure 4.3). Let $\bar{\phi}_{20}^{(1)}$ represent such a reflected ray.

$$\bar{\phi}_{20}^{(1)}(r, \alpha) = \frac{\bar{p}_1(\alpha)}{\alpha c_{111}} R_{1\ell}(\alpha) R_{11}(\alpha) h_o^{(1)}(r, \alpha) \quad (4.13)$$

and the boundary condition which will determine $R_{11}(\alpha)$ is

$$\bar{\sigma}_{r_{11}}^{(1)}(1, \alpha) + \bar{\sigma}_{r_{20}}^{(1)}(1, \alpha) = 0 \quad (4.14)$$

yielding

$$R_{11}(\alpha) = - \frac{c_{121}}{c_{111}} \quad (4.15)$$

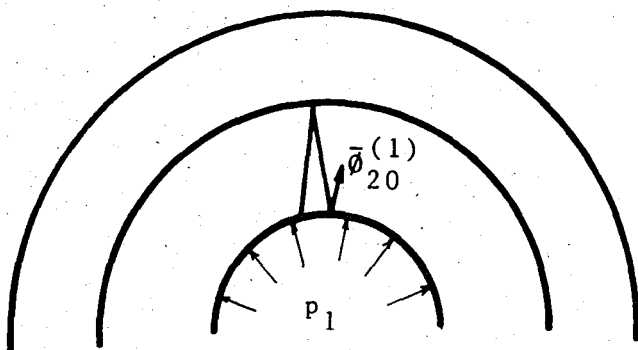


FIGURE 4.3. Converging wave after reflected at $r=1$.

Note that this reflection coefficient is exactly the same as that given by Pao and Ceranoğlu (8) for a single layered shell.

In a similar manner, we can define the reflection coefficients R_{2b} and $R_{2\ell}$ and the transmission coefficient T_{21} . Going through a similar procedure, we get

$$R_{2b}(\alpha) = -\frac{c_{21b}}{c_{22b}} \quad (4.16)$$

$$R_{2\ell}(\alpha) = \frac{c_{12\ell}^d d_{22\ell} - \beta_2 \eta_2 c_{22\ell}^d d_{12\ell}}{\beta_2 \eta_2 c_{21\ell}^d d_{12\ell} - c_{12\ell}^d d_{21\ell}} \quad (4.17)$$

$$T_{21}(\alpha) = \frac{\beta_2 \eta_2 (c_{21\ell}^d d_{22\ell} - c_{22\ell}^d d_{21\ell})}{\beta_2 \eta_2 c_{21\ell}^d d_{12\ell} - c_{12\ell}^d d_{21\ell}} \quad (4.18)$$

Note that R_{2b} is the reflection coefficient at the outer surface. $R_{2\ell}$ and T_{21} are the reflection and transmission coefficients for those waves that are impinging on the interface while travelling inside the second layer. Note that consideration of the pressure applied to the outer surface would yield exactly the same reflection and transmission coefficients.

A complete list of the reflection and transmission coefficients is given in Table 4.1.

$$R_{11}(\alpha) = \frac{(\alpha - \gamma_1)(\alpha + \gamma_1^*)}{(\alpha + \gamma_1)(\alpha - \gamma_1^*)} e^{-2i\alpha} \quad (4.19)$$

$$R_{1\ell}(\alpha) = \frac{e^{2i\alpha\ell}}{\Delta_{RT}} \{ i\beta_2 \ell^3 (1 - \beta_2 \eta_2) \alpha^3 + [(\beta_2^2 \eta_2 - 1) \ell^2 - y \beta_2 \ell^2] \alpha^2 - iy\ell(\beta_2 + 1)\alpha + y \} \quad (4.20)$$

$$T_{12}(\alpha) = \frac{e^{-i\alpha\ell(\beta_2 - 1)}}{\Delta_{RT}} \{ 2i\beta_2 \ell^3 \alpha^3 \} \quad (4.21)$$

$$T_{21}(\alpha) = \frac{e^{-i\alpha\ell(\beta_2 - 1)}}{\Delta_{RT}} \{ 2i\beta_2^2 \eta_2 \ell^3 \alpha^3 \} \quad (4.22)$$

$$R_{2\ell}(\alpha) = \frac{e^{-2i\alpha\beta_2\ell}}{\Delta_{RT}} \{ i\beta_2 \ell^3 (\beta_2 \eta_2 - 1) \alpha^3 + [(\beta_2^2 \eta_2 - 1) \ell^2 - y \beta_2 \ell^2] \alpha^2 + iy\ell(\beta_2 + 1)\alpha + y \} \quad (4.23)$$

$$R_{2b}(\alpha) = \frac{(\beta_2 b \alpha + \gamma_2)(\beta_2 b \alpha - \gamma_2^*)}{(\beta_2 b \alpha - \gamma_2)(\beta_2 b \alpha + \gamma_2^*)} e^{2i\alpha\beta_2 b} \quad (4.24)$$

TABLE 4.1. Reflection and Transmission Coefficients

In Table 4.1

$$\Delta_{RT} = i\beta_2 \ell^3 (1 + \beta_2 \eta_2) \alpha^3 + [(\beta_2^2 \eta_2 - 1) \ell^2 + y \beta_2 \ell^2] \alpha^2 + iy\ell(1 - \beta_2)\alpha + y \quad (4.25)$$

$$y = 4(\kappa_1 - \kappa_2 \eta_2)$$

$$\gamma_j = m_j + in_j, \quad \gamma_j^* = m_j - in_j \quad j=1,2 \quad (4.26)$$

$$m_j = 2\kappa_j \sqrt{(\kappa_j^{-1} - 1)} \quad n_j = 2\kappa_j \quad j=1,2 \quad (4.27)$$

C. RAY THEORY SOLUTION

In this section, the Fourier transformed normal mode solution obtained earlier will be expanded into a series, where each term will represent a spherical harmonic wave travelling inside the shell.

For easiness, we will consider the case where an internal pressure $p_1(t)$ is applied to the shell. The unknown constants in the normal mode solution can be obtained from the matrix equation,

$$\begin{bmatrix} c_{111} & c_{121} & 0 & 0 \\ 0 & 0 & c_{21b} & c_{22b} \\ d_{11\ell} & d_{12\ell} & -d_{21\ell} & -d_{22\ell} \\ c_{11\ell} & c_{12\ell} & -\beta_2 \eta_2 c_{21\ell} & -\beta_2 \eta_2 c_{22\ell} \end{bmatrix} \begin{bmatrix} A_1 \\ B_1 \\ A_2 \\ B_2 \end{bmatrix} = \begin{bmatrix} \frac{\bar{p}_1(\alpha)}{\alpha} \\ 0 \\ 0 \\ 0 \end{bmatrix} \quad (4.28)$$

Denoting the coefficient matrix by $[M]$,

$$[M] = \begin{bmatrix} c_{111} & c_{121} & 0 & 0 \\ 0 & 0 & c_{21b} & c_{22b} \\ d_{11\ell} & d_{12\ell} & -d_{21\ell} & -d_{22\ell} \\ c_{11\ell} & c_{12\ell} & -\beta_2 \eta_2 c_{21\ell} & -\beta_2 \eta_2 c_{22\ell} \end{bmatrix} \quad (4.29)$$

the solution of Eq (4.28) can be written as

$$\begin{bmatrix} A_1 \\ B_1 \\ A_2 \\ B_2 \end{bmatrix} = [M]^{-1} \begin{bmatrix} \frac{\bar{p}_1(\alpha)}{\alpha} \\ 0 \\ 0 \\ 0 \end{bmatrix} \quad (4.30)$$

Instead of calculating the matrix $[M]^{-1}$ one can expand it into a series form by writing (15)

$$\begin{aligned} [M]^{-1} &= \begin{bmatrix} I & E \\ F & I \end{bmatrix}^{-1} = \begin{bmatrix} I & 0 \\ 0 & I \end{bmatrix} - \begin{bmatrix} 0 & -E \\ -F & 0 \end{bmatrix}^{-1} \\ &= [I] + \sum_{n=1}^{\infty} \begin{bmatrix} 0 & -E \\ -F & 0 \end{bmatrix}^n \end{aligned} \quad (4.31)$$

where I is the identity matrix, 0 is the null matrix and E and F are the submatrices.

It would be more convenient to write the matrix equation given in Eq (4.28) in a slightly different form

$$\begin{bmatrix} 1 & 0 & -R_{11} & 0 \\ 0 & 1 & -\frac{T_{12}}{R_{1\ell}} & -U_2 \\ -U_1 & -\frac{T_{21}}{R_{2\ell}} & 1 & 0 \\ 0 & -R_{2b} & 0 & 1 \end{bmatrix} \begin{bmatrix} A_1 \\ A_2 \\ B_1 \\ B_2 \end{bmatrix} = \begin{bmatrix} \frac{\bar{p}_1(\alpha)}{\alpha c_{111}} \\ 0 \\ 0 \\ 0 \end{bmatrix} \quad (4.32)$$

where

$$U_1 = \frac{\beta_2 \eta_2 c_{22\ell} d_{11\ell} - c_{11\ell} d_{22\ell}}{c_{12\ell} d_{22\ell} - \beta_2 \eta_2 c_{22\ell} d_{12\ell}} \quad (4.33)$$

$$U_2 = \frac{\beta_2 \eta_2 c_{22\ell} d_{11\ell} - c_{11\ell} d_{22\ell}}{c_{11\ell} d_{21\ell} - \beta_2 \eta_2 c_{21\ell} d_{11\ell}} \quad (4.34)$$

Expanding the new coefficient matrix of Eq (4.32) into a series and solving the equation, the constants are found as

$$\begin{aligned} A_1 = \frac{\bar{p}_1(\alpha)}{\alpha c_{111}} & \left[1 + R_{11} X_1 + R_{11}^2 X_1^2 + R_{11}^3 X_1^3 + \dots \right. \\ & \left. + T_{12} R_{2b} T_{21} R_{11} \frac{X_1}{R_{1\ell}} \frac{X_2}{R_{2\ell}} + \dots \right] \quad (4.35) \end{aligned}$$

where

$$X_1 = U_1 \left[1 + \sum_{j=1}^{\infty} \left(\frac{T_{12} T_{21}}{R_{1\ell} R_{2\ell}} \right)^j \right] \quad (4.36)$$

$$X_2 = U_2 \left[1 + \sum_{j=1}^{\infty} \left(\frac{T_{12} T_{21}}{R_{1\ell} R_{2\ell}} \right)^j \right] \quad (4.37)$$

$$B_1 = \frac{\bar{p}_1(\alpha)}{\alpha c_{111}} \left[X_1 + R_{11} X_1^2 + R_{11}^2 X_1^3 + \dots \right. \\ \left. + T_{12} R_{2b} T_{21} \frac{X_1}{R_{1\ell}} \frac{X_2}{R_{2\ell}} + \dots \right] \quad (4.38)$$

$$A_2 = \frac{\bar{p}_1(\alpha)}{\alpha c_{111}} \left[T_{12} \frac{X_1}{R_{1\ell}} + T_{12} R_{2b} X_2 \frac{X_1}{R_{1\ell}} + \dots \right. \\ \left. + \frac{X_1^2}{R_{1\ell}} R_{11} T_{12} R_{2b} X_2 + \dots \right] \quad (4.39)$$

$$B_2 = \frac{\bar{p}_1(\alpha)}{\alpha c_{111}} \left[T_{12} R_{2b} \frac{X_1}{R_{1\ell}} + T_{12} R_{2b}^2 X_2 \frac{X_1}{R_{1\ell}} + \dots \right. \\ \left. + \frac{X_1^2}{R_{1\ell}} R_{11} T_{12} R_{2b} + \dots + T_{12}^2 R_{2b} T_{21} R_{11} \frac{X_1^2}{R_{1\ell}^2} + \dots \right] \quad (4.40)$$

The terms X_1 and X_2 appearing in series form in the above expressions are equal to $R_{1\ell}(\alpha)$ and $R_{2\ell}(\alpha)$, respectively. These are given in Appendix B.

Inserting A_1 , B_1 , A_2 and B_2 into the solution given in Eq (3.2), we finally obtain the ray theory solution in the form

$$\bar{\Phi}^{(1)}(r, \alpha) = \frac{\bar{p}_1(\alpha)}{\alpha c_{111}} \left[1 + R_{11} R_{1\ell} + R_{11}^2 R_{1\ell}^2 + R_{11}^3 R_{1\ell}^3 + \dots \right. \\ \left. + T_{12} R_{2b} T_{21} R_{11} + \dots \right] h_o^{(1)}(r\alpha) \\ + \frac{\bar{p}_1(\alpha)}{\alpha c_{111}} \left[R_{1\ell} + R_{11} R_{1\ell}^2 + R_{11}^2 R_{1\ell}^3 + \dots \right. \\ \left. + T_{12} R_{2b} T_{21} + T_{12} R_{2b} T_{21} R_{11} R_{1\ell} + \dots \right] h_o^{(2)}(r\alpha) \quad (4.41)$$

$$\begin{aligned}
\bar{\Phi}^{(2)}(r, \alpha) = & \frac{\bar{p}_1(\alpha)}{\alpha c_{111}} \left[T_{12} + T_{12}R_{2b}R_{2\ell} + \dots + R_{1\ell}R_{11}T_{12}R_{2b}R_{2\ell} \right. \\
& \left. + \dots + T_{12}^2R_{2b}T_{21}R_{11} + \dots \right] h_o^{(1)}(\beta_2 r \alpha) \\
& + \frac{\bar{p}_1(\alpha)}{\alpha c_{111}} \left[T_{12}R_{2b} + T_{12}R_{2b}^2R_{2\ell} + \dots \right. \\
& \left. + R_{1\ell}R_{11}T_{12}R_{2b} + \dots + T_{12}^2R_{2b}T_{21}R_{11} \right. \\
& \left. + \dots \right] h_o^{(2)}(\beta_2 r \alpha) \quad (4.42)
\end{aligned}$$

Note that the above expressions are only due to an internally applied pressure. Each term in the series represents a spherical harmonic wave, which can be seen by writing the expressions in their complete form with $e^{-i\alpha t}$ appended.

The complete series expressions for both internal and external pressures can be written in the form of:

$$\bar{\Phi}^{(i)}(r, \alpha) = \sum_{j=0}^{\infty} \left[\bar{\phi}_{jk}^{(i)}(r, \alpha) + \bar{\Psi}_{jk}^{(i)}(r, \alpha) \right] \quad (4.43)$$

where $\bar{\phi}_{jk}^{(i)}(r, \alpha)$ are the waves generated by the internal pressure $\bar{p}_1(\alpha)$, and $\bar{\Psi}_{jk}^{(i)}$ are the waves due to external pressure $\bar{p}_2(\alpha)$.

Note that $i=1,2$ shows the layer number, $j=0,1,2,3,\dots$ is the ray index, and $k=0,1$ represents outgoing or incoming ray respectively.

The initial rays for an observation point in the first layer due to internal pressure were given by Eqs (4.6) and (4.7). However, if the observation point is in the second layer, then

some of the first few rays are (Figure 4.4)

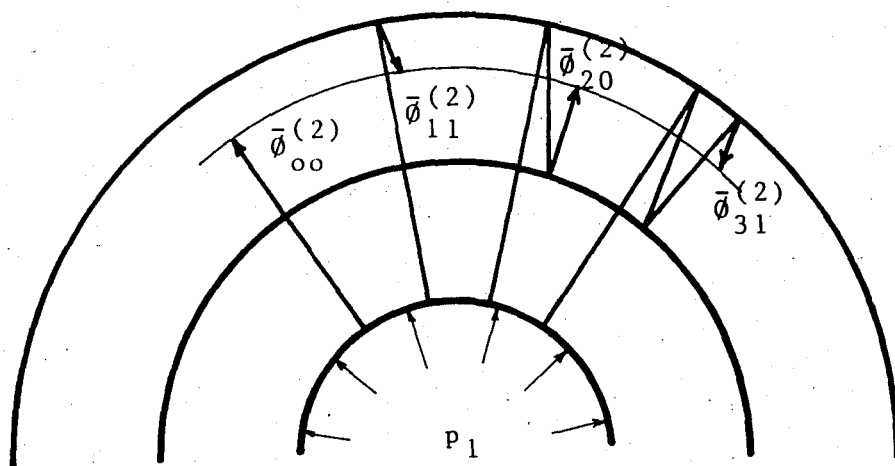


FIGURE 4.4. Initial rays in the second layer.

$$\bar{\phi}_{00}^{(2)}(r, \alpha) = \frac{\bar{p}_1(\alpha)}{\alpha c_{111}} T_{12}(\alpha) h_o^{(1)}(\beta_2 r \alpha) \quad (4.44)$$

$$\bar{\phi}_{11}^{(2)}(r, \alpha) = \frac{\bar{p}_1(\alpha)}{\alpha c_{111}} T_{12}(\alpha) R_{2b}(\alpha) h_o^{(2)}(\beta_2 r \alpha) \quad (4.45)$$

$$\bar{\phi}_{20}^{(2)}(r, \alpha) = \frac{\bar{p}_1(\alpha)}{\alpha c_{111}} T_{12}(\alpha) R_{2b}(\alpha) R_{2\ell}(\alpha) h_o^{(1)}(\beta_2 r \alpha) \quad (4.46)$$

$$\bar{\phi}_{31}^{(2)}(r, \alpha) = \frac{\bar{p}_1(\alpha)}{\alpha c_{111}} T_{12}(\alpha) R_{2b}^2(\alpha) R_{2\ell}(\alpha) h_o^{(2)}(\beta_2 r \alpha) \quad (4.47)$$

The general expression for a ray generated by an internal pressure coming to a receiver point in the i -th layer with the ray index, j , can be written in the form of

$$\bar{\phi}_{jk}^{(i)}(r, \alpha) = \frac{\bar{p}_1(\alpha)}{\alpha c_{111}} R_{1\ell}^m T_{12}^n R_{2b}^p R_{2\ell}^q T_{21}^r R_{11}^s h_o^{(k+1)}(\beta_i r \alpha) \quad (4.48)$$

where $m, n, p, q, r, s = 0, 1, 2, \dots$ show the number of reflections and transmissions the ray has gone through, and $k=0, 1$ for outgoing and incoming rays respectively.

Similar terms can be written for the rays $\bar{\psi}_{jk}^{(i)}(r, \alpha)$ which are generated by the pressure $\bar{p}_2(\alpha)$ at the surface $r=b$.

Taking the inverse transform of each wave, we obtain the complete solution as

$$\phi^{(i)}(r, t) = \frac{1}{2\pi} \sum_{j=0}^{\infty} \int_{-\infty+i\epsilon}^{\infty+i\epsilon} \left[\bar{\phi}_{jk}^{(i)}(r, \alpha) + \bar{\psi}_{jk}^{(i)}(r, \alpha) \right] e^{-i\alpha t} d\alpha \quad (4.49)$$

Each term of the series in Eq (4.49) is called a ray-integral or a ray of the transient wave solution.

The inverse transforms of the fundamental rays given in Eqs (4.6), (4.7), (4.44) and (4.45) are evaluated analytically, whereas the higher order terms are calculated using the convolution integral as will be explained in Section B of Chapter V.

V. TRANSIENT SOLUTION FOR AN INTERNAL PRESSURE

A. PROBLEM AND INITIAL RAYS

Consider the case of a suddenly applied uniform pressure, p_0 , at the internal surface, thus,

$$\begin{aligned} p_1(t) &= p_0 H(t) \\ p_2(t) &= 0 \end{aligned} \quad (5.1)$$

where $H(t)$ is the Heaviside's unit step function. The Fourier transforms of the above expressions are obtained from Eq (3.1.a) as,

$$\begin{aligned} \bar{p}_1(\alpha) &= \frac{ip_0}{\alpha} \quad (\text{Im}\alpha > 0) \\ \bar{p}_2(\alpha) &= 0 \end{aligned} \quad (5.2)$$

Since $\bar{p}_2(\alpha) = 0$, all $\bar{\psi}_{jk}^{(i)}(r, \alpha)$ are zero.

For a point of observation located in the first layer, the first fundamental ray is, Eq (4.6),

$$\bar{\phi}_{oo}^{(1)}(r, \alpha) = \frac{ip_0 e^{-i\alpha(1-r)}}{\alpha r(\alpha + \gamma_1)(\alpha - \gamma_1^*)} \quad (5.3)$$

with the inverse Fourier transform

$$\phi_{oo}^{(1)}(r, t) = \frac{ip_o}{2\pi r} \int_{-\infty+i\epsilon}^{\infty+i\epsilon} \frac{e^{-i\alpha(t-r+1)}}{\alpha(\alpha+\gamma_1)(\alpha-\gamma_1^*)} d\alpha \quad (5.4)$$

The above integral will be evaluated by connecting the path of integration by a closed contour as shown in Figure 5.1. Note that the above integral has three simple poles inside the contour of integration. These singularities are

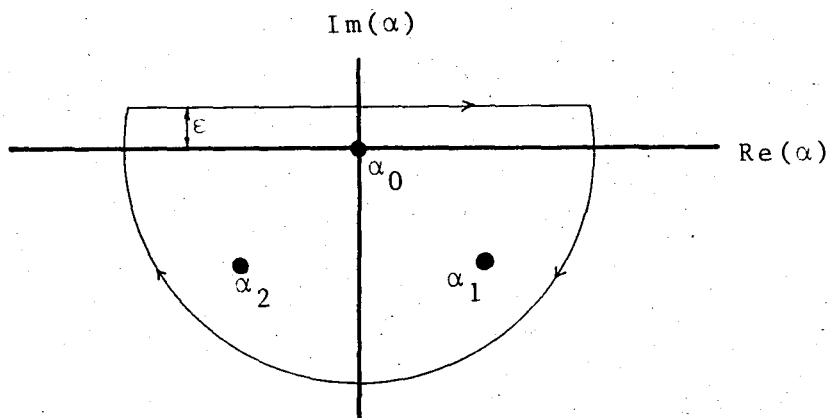


FIGURE 5.1. Path of integration for $\bar{\phi}_{oo}^{(1)}(r, \alpha)$.

$$\alpha_o = 0 \quad \alpha_1 = \gamma_1^* \quad \alpha_2 = -\gamma_1 \quad (5.5)$$

where γ_1 and γ_1^* were defined by Eq (4.26).

Applying the residue theorem, we get

$$\phi_{oo}^{(1)}(r, t) = \frac{p_o}{r} \sum_{j=0}^2 \frac{e^{-i\alpha_j(t-r+1)} H(t-r+1)}{3\alpha_j^2 + 8i\kappa_1\alpha_j - 4\kappa_1} \quad (5.6)$$

The step function in the form of $H(t-t_a)$, in Eq (5.6), defines the arrival time of the ray. Contribution from this ray is zero prior to its arrival time, t_a .

Inverse transforms of the first incoming wave, $\bar{\phi}_{11}^{(1)}(r, \alpha)$ for the first layer, and the initial outgoing and incoming waves, $\bar{\phi}_{oo}^{(2)}(r, \alpha)$ and $\bar{\phi}_{11}^{(2)}$, coming to the receiver point in the second layer can be obtained in a similar way.

The ray paths of the above mentioned rays, $\phi_{oo}^{(1)}$, $\phi_{11}^{(1)}$, $\phi_{oo}^{(2)}$ and $\phi_{11}^{(2)}$ are illustrated in Figure 5.2.

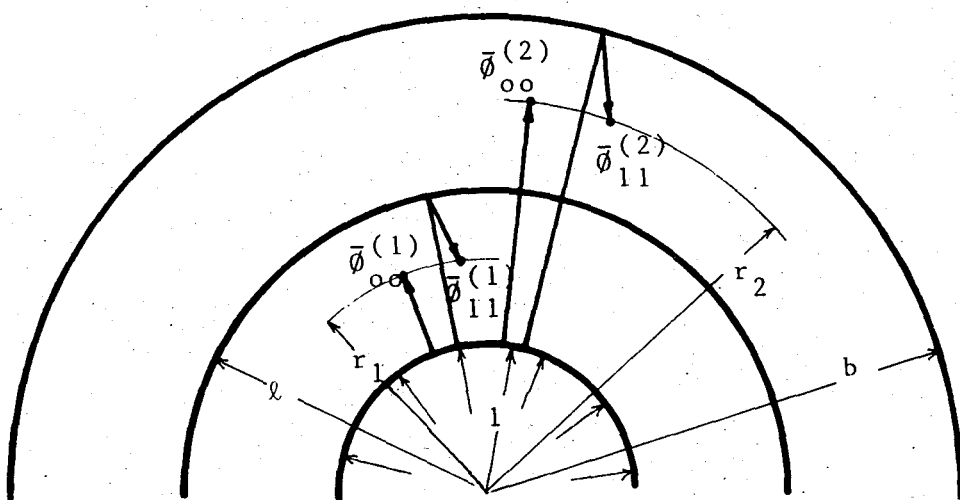


FIGURE 5.2. Paths of the fundamental rays.

B. HIGHER ORDER RAYS

After completing the inversions of the fundamental rays, the higher order terms in the series solution can be obtained by a convolution integral.

$$\phi_{jk}^{(i)}(r, t) = q(t) * \phi_{j-2, k}^{(i)}(r, t) = \int_{-\infty}^{\infty} q(\tau) \phi_{j-2, k}^{(i)}(r, t-\tau) d\tau \quad (5.7)$$

where

$$\phi_{j-2, k}^{(i)}(r, t) = \frac{1}{2\pi} \int_{-\infty+i\epsilon}^{\infty+i\epsilon} \bar{\phi}_{j-2}^{(i)}(r, \alpha) e^{-i\alpha t} d\alpha$$

and $q(t)$ is the inverse transform of the product of the reflection-transmission coefficients which are appended to the Fourier transformed expressions of the former ray used in convolution. As will be seen from Eqs (4.41) and (4.42), in order to determine the successive rays using convolution, we need to find the inverse Fourier transforms of terms such as $R_{11}R_{1\ell}$, $R_{2b}R_{2\ell}$ and $T_{12}R_{2b}T_{21}R_{11}$ which is further obtained by convoluting the inverse transforms of $T_{12}R_{2b}$ and $T_{21}R_{11}$.

As an example, let's find the ray $\phi_{20}^{(1)}(r, t)$ (Fig. 4.3), by convolution

$$\phi_{20}^{(1)}(r, t) = q(t) * \phi_{00}^{(1)}(r, t) = \int_{-\infty}^{\infty} q(\tau) \phi_{00}^{(1)}(r, t-\tau) d\tau \quad (5.8)$$

where

$$q(t) = \frac{1}{2\pi} \int_{-\infty+i\epsilon}^{\infty+i\epsilon} R_{11}(\alpha) R_{1\ell}(\alpha) e^{-i\alpha t} d\alpha \quad (5.9)$$

and $\phi_{00}^{(1)}(r, t)$ is the ray found in Eq (5.6).

Using Eqs (4.19) and (4.20), we can write

$$q(t) = \frac{1}{2\pi} \int_{-\infty+i\epsilon}^{\infty+i\epsilon} \left\{ f_1 + \frac{n_{14}\alpha^4 + n_{13}\alpha^3 + n_{12}\alpha^2 + n_{11}\alpha + n_{10}}{(\alpha + \gamma_1)(\alpha - \gamma_1^*) \Delta_{RT}} \right\} e^{-i\alpha(t+2-2\ell)} d\alpha \quad (5.10)$$

where

$$f_1 = \frac{1 - \beta_2 \eta_2}{1 + \beta_2 \eta_2}$$

Δ_{RT} is the term given in Eq (4.25)

$$n_{10} = - (1 - f_1) 4\kappa_1 y$$

$$n_{11} = 4i\kappa_1 y \left[(1 + f_1)(\ell - 1) + (1 - f_1)\ell\beta_2 \right]$$

$$n_{12} = 4\kappa_1 y \ell \beta_2 (1 + f_1)(\ell - 1) - 4\kappa_1 \ell (1 - f_1) (\ell \beta_2^2 \eta_2 - \ell + y) + (1 - f_1) y$$

$$n_{13} = 4i\kappa_1 \left[(1 + f_1) (\beta_2^2 \eta_2 \ell^3 - \beta_2^2 \eta_2 \ell^2 + 1) + (1 - f_1) (y \beta_2 \ell^2 - \beta_2 \ell^3) \right] \\ - iy\ell \left[1 + f_1 + \beta_2 (1 - f_1) \right]$$

$$n_{14} = 4\kappa_1 \beta_2 \ell^3 \left[1 + f_1 - \beta_2 \eta_2 (1 - f_1) \right] + (1 - f_1) (\beta_2^2 \eta_2 \ell^2 - \ell^2) - (1 + f_1) y \beta_2 \ell^2$$

$$\text{and } y = 4(\kappa_1 - \kappa_2 \eta_2)$$

The first term in the curly bracket gives rise to a delta function, and the second term can be evaluated by using a path of

integration similar to the one shown in Figure 5.1. Applying the residue theorem, we find

$$q(t) = f_1 \delta(t+2-2\ell) - i \sum_{j=1}^5 Q_1(\alpha_j) e^{-i\alpha_j(t+2-2\ell)} H(t+2-2\ell) \quad (5.11)$$

where

$$Q_1(\alpha_j) = \frac{n_{14}\alpha_j^4 + n_{13}\alpha_j^3 + n_{12}\alpha_j^2 + n_{11}\alpha_j + n_{10}}{5d_{14}\alpha_j^4 + 4d_{13}\alpha_j^3 + 3d_{12}\alpha_j^2 + 2d_{11}\alpha_j + d_{10}}$$

$$d_{10} = 4i\kappa_1 y (1 - \ell + \beta_2 \ell)$$

$$d_{11} = -4\kappa_1 \left[y\ell(1-\beta_2) + (\beta_2^2 \eta_2 - 1)\ell^2 + y\beta_2 \ell^2 \right] + y$$

$$d_{12} = iy\ell(1-\beta_2) + i4\kappa_1(\beta_2^2 \eta_2 - 1)\ell^2 - 4i\kappa_1 \beta_2 \ell^3 (1 + \beta_2 \eta_2)$$

$$d_{13} = (\beta_2^2 \eta_2 - 1)\ell^2 + y\beta_2 \ell^2 - 4\kappa_1 \beta_2 \ell^3 (1 + \beta_2 \eta_2)$$

$$d_{14} = i\beta_2 \ell^3 (1 + \beta_2 \eta_2)$$

The singularities of Eq (5.11) are $\alpha_1 = -\gamma_1$, $\alpha_2 = \gamma_1^*$, where γ_1 and γ_1^* were defined in Eq (4.26), and $\alpha_{3,4,5}$ are the roots of Δ_{RT} (Eq. (4.25)).

$R_{2b}R_{2\ell}(t)$ term, which is necessary for some higher order rays in convolution, can be obtained through a similar procedure as

$$R_{2b}R_{2\ell}(t) = f_2 \delta(t-2\beta_2 b + 2\beta_2 \ell) - i \sum_{j=1}^5 Q_2(\alpha_j) e^{-i\alpha_j(t-2\beta_2 b + 2\beta_2 \ell)} H(t-2\beta_2 b + 2\beta_2 \ell) \quad (5.12)$$

where

$$Q_2(\alpha_j) = \frac{n_{24}\alpha_j^4 + n_{23}\alpha_j^3 + n_{22}\alpha_j^2 + n_{21}\alpha_j + n_{20}}{5d_{24}\alpha_j^4 + 4d_{23}\alpha_j^3 + 3d_{22}\alpha_j^2 + 2d_{21}\alpha_j + d_{20}}$$

$$f_2 = \frac{\beta_2 \eta_2 - 1}{\beta_2 \eta_2 + 1}$$

$$n_{20} = (f_2 - 1) 4\kappa_2 y$$

$$n_{21} = 4i\kappa_2 y \left[(1+f_2)(\beta_2 b - \ell\beta_2) - (1-f_2)\ell \right]$$

$$n_{22} = 4\kappa_2 \ell \left[(1+f_2)(y\beta_2 \ell - \beta_2 by) - (1-f_2)(\beta_2^2 by + \ell(\beta_2^2 \eta_2 - 1)) \right] + (1-f_2)\beta_2^2 b^2 y$$

$$n_{23} = 4i\kappa_2 \beta_2 \left[(1+f_2)(b\ell^2(\beta_2^2 \eta_2 - 1) + \ell^3) - (1-f_2)(\beta_2 by \ell^2 + \beta_2 \eta_2 \ell^3) \right] \\ + iy\ell\beta_2^2 b^2 \left[(1+f_2)b + 1 - f_2 \right]$$

$$n_{24} = 4\kappa_2 \beta_2^2 b \ell^3 \left[1 - f_2 - (1+f_2)\beta_2 \eta_2 \right] + \beta_2^2 b^2 \ell^2 \left[(1-f_2)(\beta_2^2 \eta_2 - 1) - (1+f_2)y\beta_2 \right]$$

$$d_{20} = -4i\kappa_2 y (\beta_2 b + \ell - \ell\beta_2)$$

$$d_{21} = 4\kappa_2 \ell \left[\beta_2 by(1-\beta_2) - \ell(\beta_2^2 \eta_2 - 1 + y\beta_2) \right] + \beta_2^2 b^2 y$$

$$d_{22} = -4i\kappa_2 \beta_2 \left[b\ell^2(\beta_2^2 \eta_2 - 1 + y\beta_2) + \ell^3(1 + \beta_2 \eta_2) \right] + iy\ell\beta_2^2 b^2 (1 - \beta_2)$$

$$d_{23} = \ell^2 \beta_2^2 b^2 (\beta_2^2 \eta_2 - 1 + y\beta_2) + 4\kappa_2 \beta_2^2 b \ell^3 (1 + \beta_2 \eta_2)$$

$$d_{24} = i\beta_2^3 b^2 \ell^3 (1 + \beta_2 \eta_2)$$

The singularities of Eq (5.12) are $\alpha_1 = \gamma_2/\beta_2 b$, $\alpha_2 = -\gamma_2^*/\beta_2 b$ and $\alpha_{3,4,5}$ are the roots of Δ_{RT} .

$T_{12}R_{2b}T_{21}R_{11}(t)$ term is evaluated convoluting $T_{12}R_{2b}(t)$ and $T_{21}R_{11}(t)$ and obtained in the form of

$$\begin{aligned}
 T_{12}R_{2b}T_{21}R_{11}(t) = & f_3 f_4 \delta(t-t_a) - i \left[f_4 \sum_{k=1}^5 Q_3(\alpha_k) e^{-i\alpha_k(t-t_a)} \right. \\
 & + f_3 \sum_{j=1}^5 Q_4(\alpha_j) e^{-i\alpha_j(t-t_a)} \\
 & + \sum_{j=1}^5 Q_4(\alpha_j) \sum_{k=1}^5 Q_3(\alpha_k) \frac{1}{(\alpha_j - \alpha_k)} \left(e^{-i\alpha_j(t-t_a)} \right. \\
 & \left. \left. - e^{-i\alpha_k(t-t_a)} \right) \right] H(t-t_a) \quad (5.13)
 \end{aligned}$$

where

$$t_a = 2\beta_2(b-l) + 2(l-1)$$

$$f_3 = \frac{2}{1+\beta_2\eta_2} \quad f_4 = \frac{2\beta_2\eta_2}{1+\beta_2\eta_2}$$

$$Q_3(\alpha_k) = \frac{n_{34}\alpha_k^4 + n_{33}\alpha_k^3 + n_{32}\alpha_k^2 + n_{31}\alpha_k + n_{30}}{5d_{14}\alpha_k^4 + 4d_{13}\alpha_k^3 + 3d_{12}\alpha_k^2 + 2d_{11}\alpha_k + d_{10}}$$

$$Q_4(\alpha_j) = \frac{n_{44}\alpha_j^4 + n_{43}\alpha_j^3 + n_{42}\alpha_j^2 + n_{41}\alpha_j + n_{40}}{5d_{24}\alpha_j^4 + 4d_{23}\alpha_j^3 + 3d_{22}\alpha_j^2 + 2d_{21}\alpha_j + d_{20}}$$

$$n_{30} = 4f_3\kappa_1y$$

$$n_{31} = 4if_3\kappa_1y \left[\ell(1 - \beta_2) - 1 \right]$$

$$n_{32} = 4f_3\kappa_1 \left[\ell^2(\beta_2^2\eta_2 - 1) + \beta_2\ell^2y + y\ell(1 - \beta_2) \right] - f_3y$$

$$n_{33} = 4if_3\kappa_1 \left[\beta_2\ell^3 - \ell^2(\beta_2^2\eta_2 - 1) - y\beta_2\ell^2 \right] - if_3y\ell(1 - \beta_2) - i(8 - 4f_3)\kappa_1\beta_2^2\eta_2\ell^3$$

$$n_{34} = -f_3 \left[\ell^2(\beta_2^2\eta_2 - 1) + y\beta_2\ell^2 - 4\kappa_1\beta_2\ell^3 \right] + (8 + 4f_3)\kappa_1\beta_2^2\eta_2\ell^3$$

The denominator of Q_3 is the same of Q_1 in Eq (5.11), and also the singularities are the same of Eq (5.11), too.

$$n_{40} = 4f_4\kappa_2y$$

$$n_{41} = 4if_4\kappa_2y \left[\ell(1 - \beta_2) + \beta_2b \right]$$

$$n_{42} = 4f_4\kappa_2 \left[\ell^2(\beta_2^2\eta_2 - 1) + \beta_2\ell^2y - \beta_2b\ell y(1 - \beta_2) \right] - f_4\beta_2^2b^2y$$

$$n_{43} = 4if_4\kappa_2 \left[\beta_2^2\eta_2\ell^3 - \ell^2\beta_2b(\beta_2^2\eta_2 - 1 + y\beta_2) \right] - if_4y\ell\beta_2^2b^2(1 - \beta_2) - i(8 - 4f_4)\kappa_2\beta_2\ell^3$$

$$n_{44} = -f_4 \left[\ell^2\beta_2^2b^2(\beta_2^2\eta_2 - 1 + y\beta_2) + 4\kappa_2\beta_2^3\eta_2b\ell^3 \right] - (8 + 4f_4)\kappa_2\beta_2^2b\ell^3$$

The denominator of Q_4 , which is equal to the denominator of Q_2 , can be seen in Eq (5.12), also the singularities of Q_4 being equal to the poles of Eq (5.12).

For the case $j=k$, in Eq (5.13), the last term in the bracket is replaced by

$$\sum_{j=1}^5 Q_4(\alpha_j) \sum_{k=1}^5 Q_3(\alpha_k) \left[-i(t - t_a) e^{-i\alpha_j(t - t_a)} \right] \quad (5.14)$$

Expressions like $\frac{\partial^2}{\partial t^2} \phi_{jk}^{(i)}$ and $\frac{\partial}{\partial r} \phi_{jk}^{(i)}$ which are necessary to calculate displacements and stresses due initial rays are obtained through straightforward differentiation, whereas those expressions belonging to the higher order rays are obtained through convolution. Thus, the displacements and stresses due to the first n rays are obtained from the following relations

$$u_r^{(i)}(r, t) = \sum_{j=0}^{n-1} \frac{\partial}{\partial r} \phi_{jk}^{(i)}(r, t) \quad (5.15)$$

$$\sigma_r^{(i)}(r, t) = \sum_{j=0}^{n-1} \eta_i \left[\beta_i^2 \frac{\partial^2 \phi_{jk}^{(i)}}{\partial t^2} - \left(\frac{4\kappa_i}{r} \right) \frac{\partial \phi_{jk}^{(i)}}{\partial r} \right] \quad (5.16)$$

$$\sigma_\theta^{(i)}(r, t) = \sum_{j=0}^{n-1} \eta_i \left[(1-2\kappa_i) \beta_i^2 \frac{\partial^2 \phi_{jk}^{(i)}}{\partial t^2} + \left(\frac{2\kappa_i}{r} \right) \frac{\partial \phi_{jk}^{(i)}}{\partial r} \right] \quad (5.17)$$

$i=1, 2$

VI. NUMERICAL RESULTS AND DISCUSSION

In order to illustrate the validity and practicality of the method, a sample problem has been solved. Radial and hoop stresses, and radial displacement for a thick-walled two-layered spherical shell have been calculated for the case of a suddenly applied uniform pressure, p_0 , at the internal surface.

Eqs (5.15) - (5.17) have been used throughout the stress and displacement calculations of the shell whose material properties are tabulated in Table 6.1.

Material Properties	Layer 1	Layer 2
c_i	8000 m/sec.	4000 m/sec
ρ_i	5 gr/cm ³	6 gr/cm ³
ν_i	0.3	0.25
β_i	1.	2.
η_i	1.	0.3
κ_i	0.2857143	0.333333
thickness, $i=1,2$	1.	1.

TABLE 6.1. Material Properties of the layers for the sample problem.

The initial rays ($\phi_{00}^{(i)}$, $\phi_{11}^{(i)}$; $i=1,2$) were calculated exactly whereas the higher order rays were evaluated numerically using the convolution integrals as explained in Section B of Chapter V.

In order to calculate the displacements and the stresses three computer programs have been developed. The first program calculates the number of rays existing in a given time and the number of reflection and transmission coefficients and the arrival times of each ray. The second program generates the data files containing the values of initial rays and reflection and transmission coefficients. These data files are used in the third program which generates the values for the radial displacements, radial and tangential stresses using numerical convolution integration.

The displacements and stresses due to total rays as well as for each single ray can be shown by graphs. The stresses were normalized by the applied pressure, p_0 , that is the quantities shown in the figures are the actual stresses. The time, t , is a dimensionless quantity, one unit of t being the time required for the ray to travel a distance equal to the inner radius.

The σ_θ/p_0 values of the first four individual rays at the inner surface can be seen in Figure 6.1. It is obvious that the first ray coming to a receiver point in the first shell is the same for both a layered spherical shell and a single layered one. Except the first ray, in Figure 6.1, each of the other rays

is individually diverging in time t . This is due to the exponentially growing terms in the expressions for each ray. However, when all rays are combined, the sum is convergent.

Figure 6.2 and 6.3 show the change of σ_{θ} at various radial locations in the first and second layers respectively. In the sample problem, the peak value for tangential stress was found to be 142 per cent of the applied internal pressure. For a single layered shell having the same material properties with the first layer, the peak value reached was 165 per cent of the applied pressure. (Figure 5 of (8)) The peak value occurred at the time unit of 6.8 in our sample problem whereas it had occurred at 2.8 in the single layered case.

Variation in radial stresses can be seen in Figures 6.4 and 6.5 for the locations in the first and the second shells. Note that due to a dynamic pressure radial stress changes from compression to tension as a result of multiple reflection of waves.

Figures 6.6 and 6.7 show the radial displacements in the first and second shells respectively. The peak value for radial displacement in our problem is evaluated as 1.31 unit of displacement, although for the single layered case this value was 1.70 (Figure 7 of (8)).

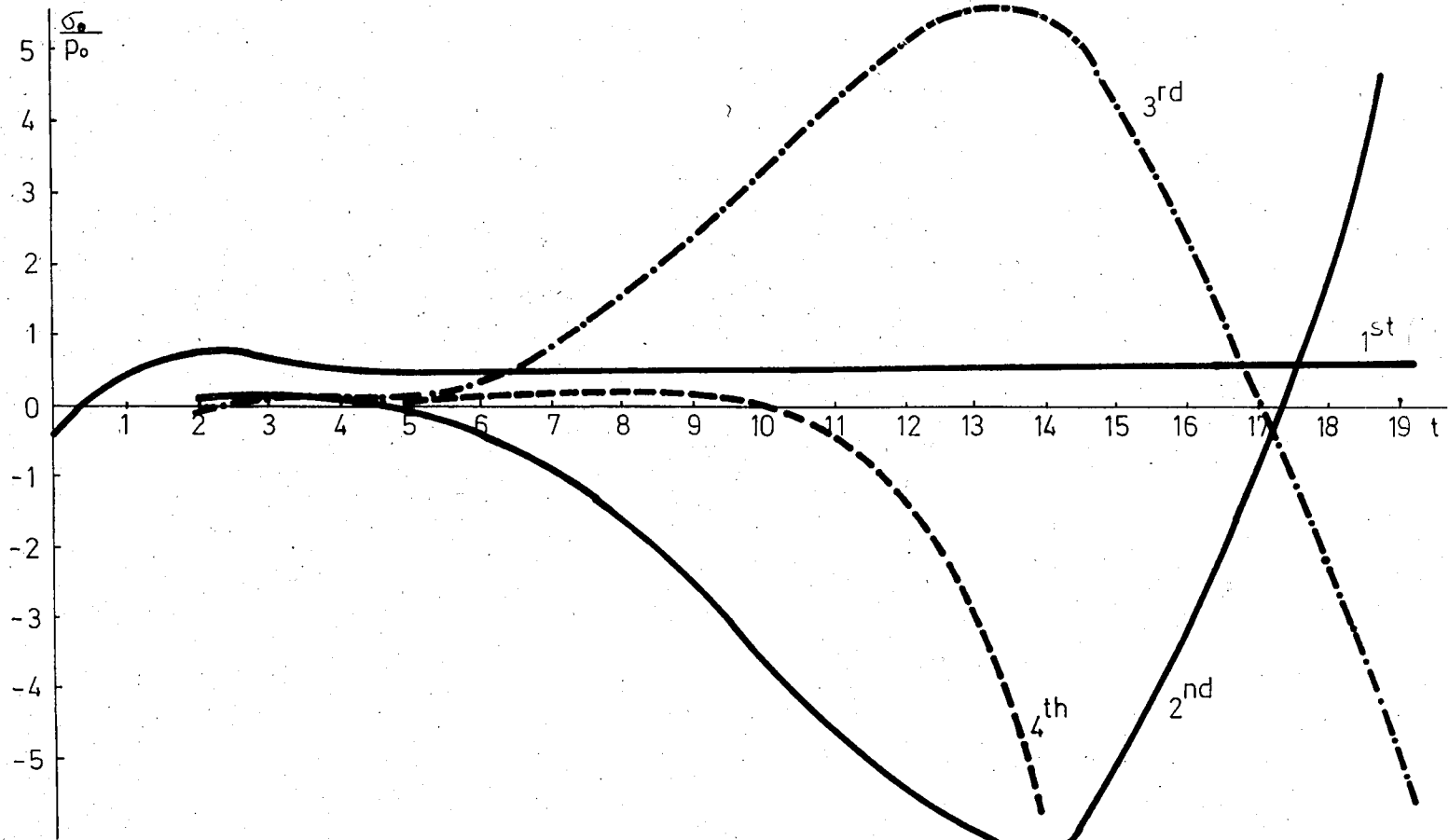


FIGURE 6.1. Values of individual rays at the inner surface ($r=1.$, $l=2.$, and $b=3.$).

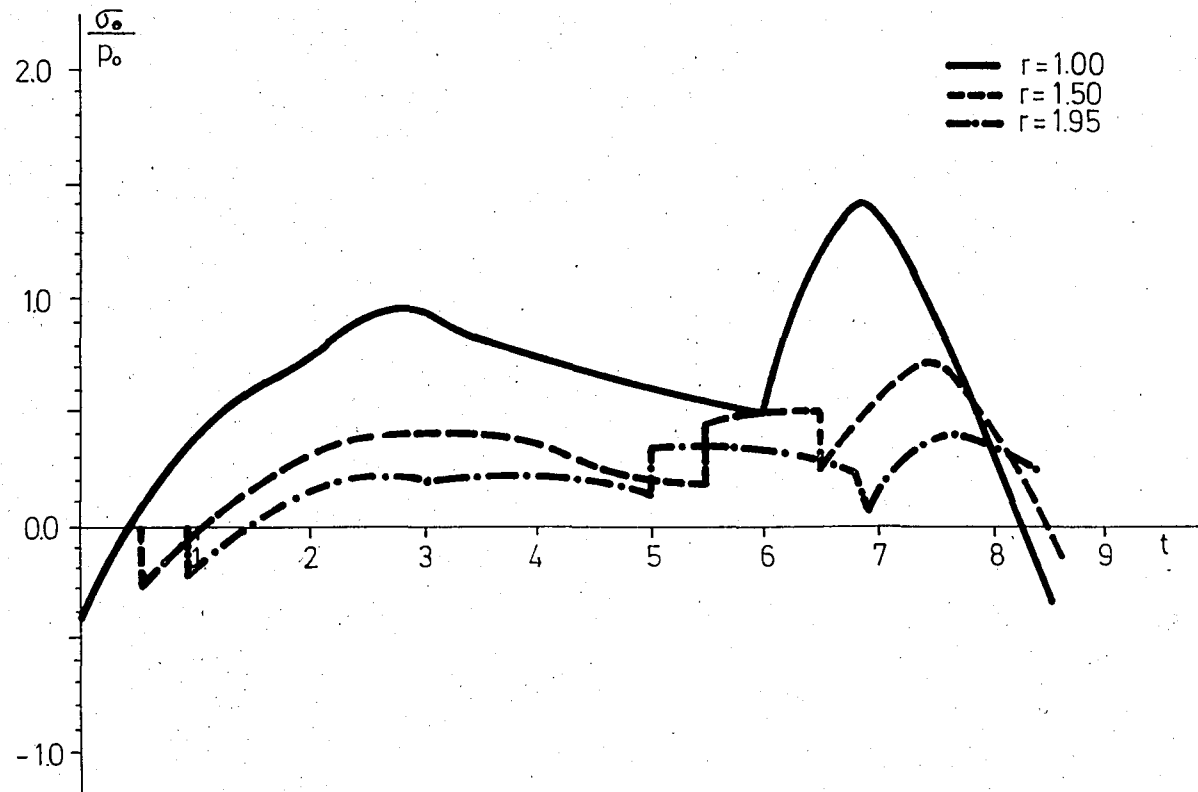


FIGURE 6.2. Variation of tangential stress with r in a two-layered shell for locations in the first layer ($\ell=2.$, $b=3.$).

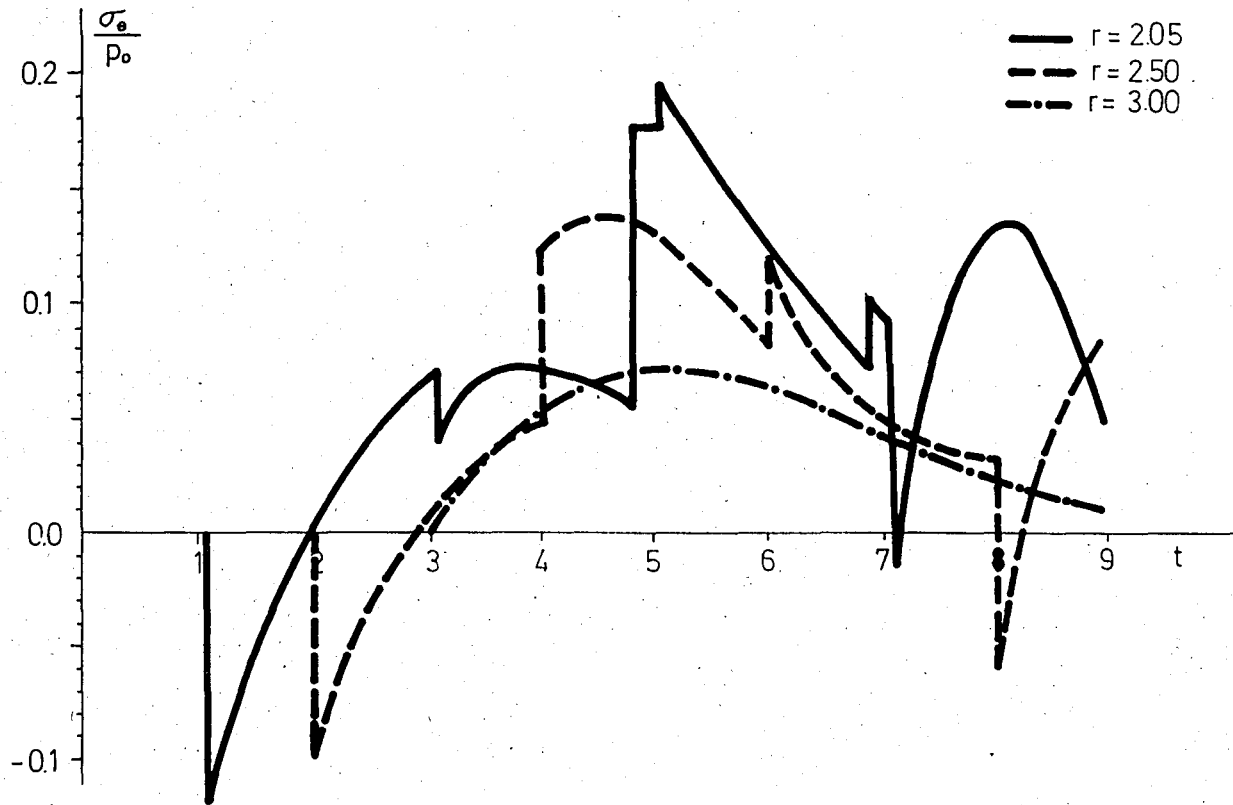


FIGURE 6.3. Variation of tangential stress with r in a two-layered shell for locations in the second layer ($\ell=2.$, $b=3.$).

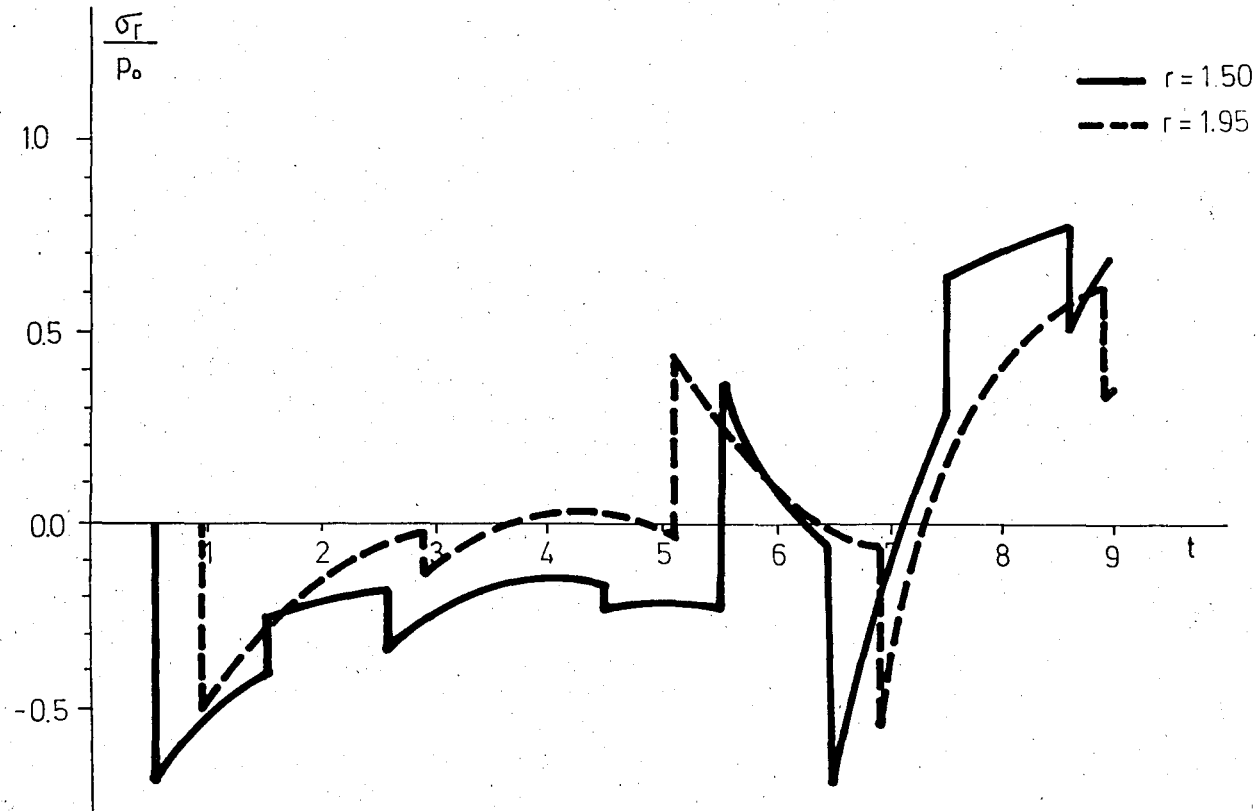


FIGURE 6.4. Variation of radial stress in a two layered shell for various locations in the first layer ($\ell=2.$, $b=3.$).

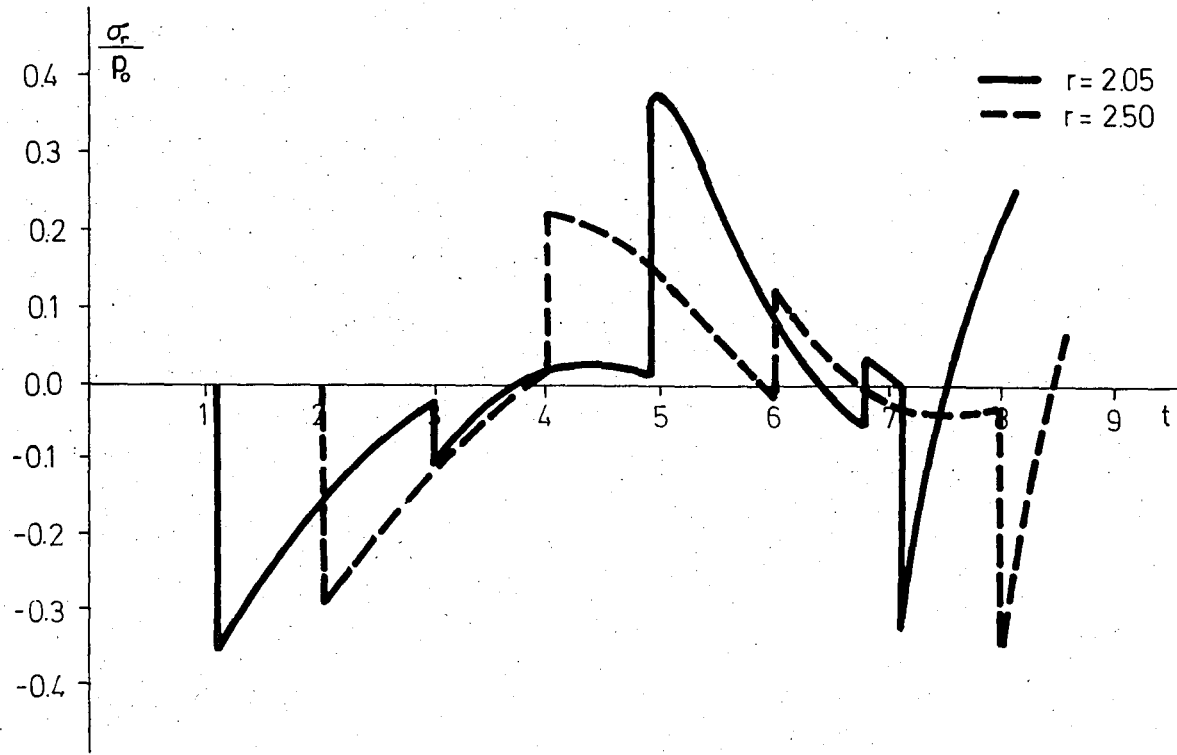


FIGURE 6.5. Variation of radial stress in a two-layered shell for various locations in the second layer ($\ell=2.$, $b=3.$).

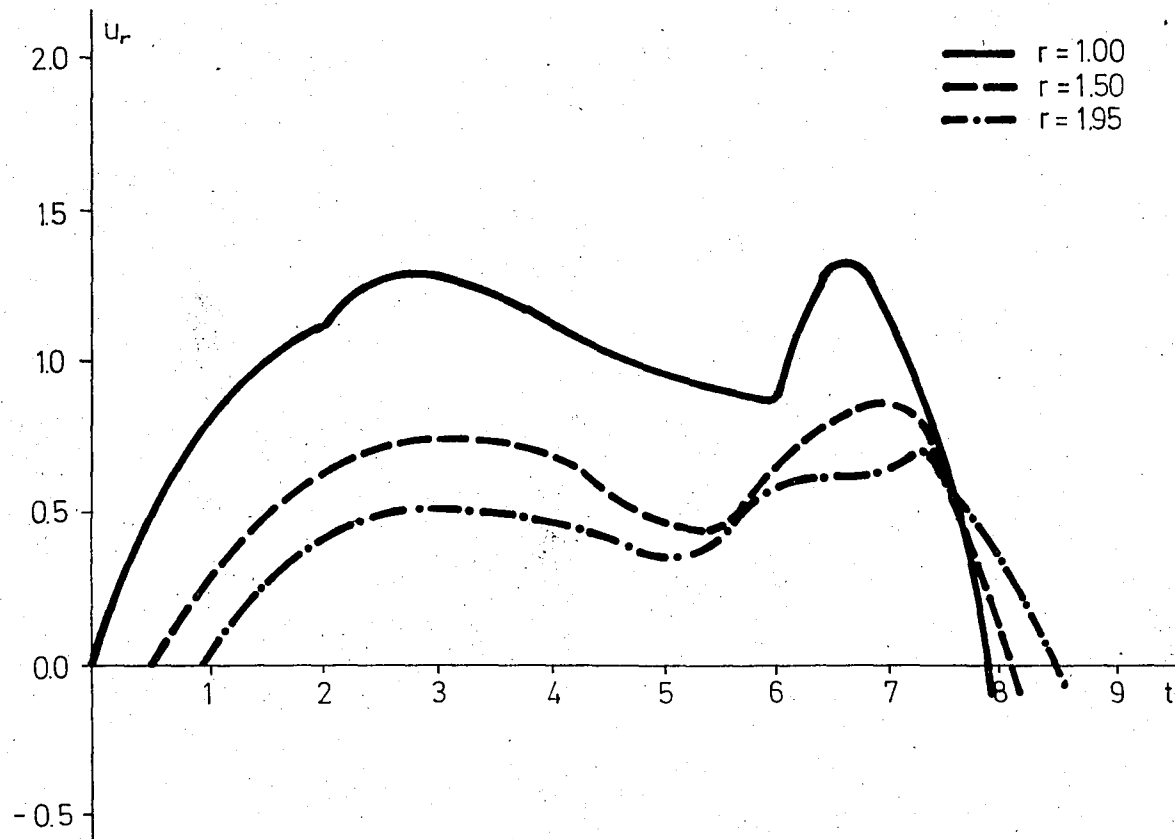


FIGURE 6.6. Radial displacement in a two-layered shell at various locations in the first layer ($\ell=2.$, $b=3.$).

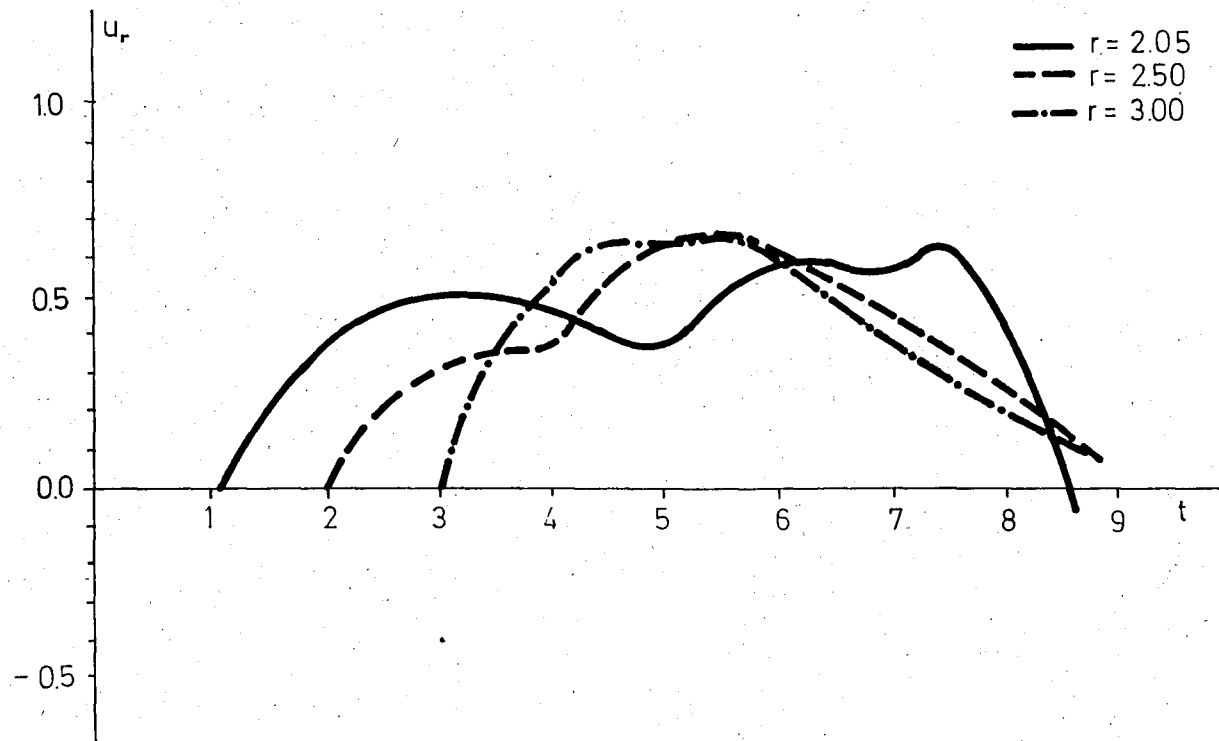


FIGURE 6.7. Radial displacement in a two-layered shell at various locations in the second layer ($\ell=2.$, $b=3.$).

VII. CONCLUSION

We have shown the ray theory gives us the exact solution for transient waves in a thick-walled layered spherical shell up to a given time of observation. The method is most effective for early time solutions of thick-walled shells because if the time of observation is large or the thickness of the shell is small the number of rays increases geometrically and the method becomes uneconomical.

In the normal mode analysis, the solution seems to be exact, but in numerical application, we need infinite number of roots in order to get the results exactly. On the other hand, our method gives the exact solution up to a given time by considering only a finite number of rays.

Practical application of layered spherical shell can be found in the design of pressure vessels, nuclear vessels, etc. Space capsules can be given as the examples for internal pressure applications, and submarines for external pressure applications.

The result of this work can be also used as a reference guide for the design of different shaped structures, e.g., layered ellipsoid shell.

Finally, we can conclude that the ray theory used in thick-walled spherical shells is an efficient method for early time solutions where exact solutions are searched.

APPENDIX A

DERIVATION OF EQUATION (3.2)

The equations of motion in terms of non-dimensional variables were given in Eq (2.21). Taking the Fourier transform of this equation, we get

$$\frac{d^2 \bar{\Phi}^{(j)}}{dr^2} + \frac{2}{r} \frac{d \bar{\Phi}^{(j)}}{dr} + \beta_j^2 \alpha^2 \bar{\Phi}^{(j)} = 0 \quad (A.1)$$

$j=1,2$

Assuming an arbitrary function

$$\bar{\chi}(r, \alpha) = r \bar{\Phi}^{(j)}(r, \alpha) \quad (A.2)$$

and inserting in Eq (A.1), we obtain

$$\frac{d^2 \bar{\chi}}{dr^2} + \beta_j^2 \alpha^2 \bar{\chi} = 0 \quad (A.3)$$

which has a solution of the form

$$\bar{\chi} = A e^{i\beta_j \alpha r} + B e^{-i\beta_j \alpha r} \quad (A.4)$$

$j=1,2$

In terms of displacement potential the solution is

$$\bar{\phi}^{(j)}(r, \alpha) = \frac{A}{r} e^{i\beta_j \alpha r} + \frac{B}{r} e^{-i\beta_j \alpha r} \quad (A.5)$$

$j=1,2$

Introducing the zeroth-order spherical Hankel functions of the first and second kinds, given in Eq (3.3), we have the final form of the Fourier transformed solution:

$$\bar{\phi}^{(j)}(r, \alpha) = A_j h_0^{(1)}(\beta_j r \alpha) + B_j h_0^{(2)}(\beta_j r \alpha) \quad (A.6)$$

$j=1,2$

APPENDIX B

SIGNIFICANCE OF X_1 AND X_2 IN A_1 , B_1 , A_2 AND B_2

The terms X_1 and X_2 appearing in the constants A_1 , B_1 , A_2 and B_2 of the solution were given in terms of U_1 and U_2 (Eqs (4.33) and (4.34)) as the following

$$X_i = U_i \left[1 + \sum_{j=1}^{\infty} \left(\frac{T_{12} \ T_{21}}{R_{1\ell} \ R_{2\ell}} \right)^j \right] \quad (4.36)$$

$$(4.37)$$

$i=1,2$

Writing the series in Eq (4.36) in the following form

$$X_1 = \frac{U_1}{1 - \frac{T_{12} \ T_{21}}{R_{1\ell} \ R_{2\ell}}} \quad (B.1)$$

and inserting the values of the above variables in terms of c_{ijk} and d_{ijk} whose definitions were given in Eq (3.7), we have

$$X_1 = \frac{\frac{\beta_2 \eta_2 c_{22\ell} d_{11\ell} - c_{11\ell} d_{22\ell}}{c_{12\ell} d_{22\ell} - \beta_2 \eta_2 c_{22\ell} d_{12\ell}}}{1 - \frac{\beta_2 \eta_2 (c_{11\ell} d_{12\ell} - c_{12\ell} d_{11\ell}) (c_{21\ell} d_{22\ell} - c_{22\ell} d_{21\ell})}{(c_{11\ell} d_{21\ell} - \beta_2 \eta_2 c_{21\ell} d_{11\ell}) (c_{12\ell} d_{22\ell} - \beta_2 \eta_2 c_{22\ell} d_{12\ell})}} \quad (B.2)$$

Evaluating the above term gives

$$X_1 = \frac{c_{11\ell} d_{21\ell} - \beta_2 \eta_2 c_{21\ell} d_{11\ell}}{\beta_2 \eta_2 c_{21\ell} d_{12\ell} - c_{12\ell} d_{21\ell}} \quad (\text{B.3})$$

which is exactly the same expression as the reflection coefficient $R_{1\ell}(\alpha)$. The same procedure can be applied to X_2 and can be found that $X_2 = R_{2\ell}(\alpha)$.

Thus, U_1 and U_2 , appearing in the matrix equation (4.32),

with the series term $\left[1 + \sum_{j=1}^{\infty} \left(\frac{T_{12} T_{21}}{R_{1\ell} R_{2\ell}} \right)^j \right]$ appended to each

represent the reflection coefficients $R_{1\ell}(\alpha)$ and $R_{2\ell}(\alpha)$, respectively.

BIBLIOGRAPHY

1. Timoshenko, S.P., and Goodier, J.N., Theory of Elasticity, McGraw Hill, New York, 1970.
2. Huth, J.H., and Cole, J.D., "Elastic-Stress Waves Produced by Pressure Loads on a Spherical Shell," ASME Journal of Applied Mechanics, Vol. 22, 1955, pp. 473-478.
3. Baker, W.E., and Allen, F.J., "The Response of Elastic Spherical Shells to Spherically Symmetric Internal Blast Loading," Proceedings of the Third U.S. National Congress of Applied Mechanics, ASME, New York, 1958, pp. 79-87.
4. Baker, W.E., "Axisymmetric Modes of Vibration of Thin Spherical Shell," The Journal of the Acoustical Society of America, Vol. 33, No. 12, 1961, pp. 1749-1758.
5. Cinelli, G., "Dynamic Vibrations and Stresses in Elastic Cylinders and Spheres," ASME Journal of Applied Mechanics, Vol. 33, 1966, pp. 825-830.
6. Rose, J.L., Chou, S.C., and Chou, P.C., "Vibration Analysis of Thick-Walled Spheres and Cylinders," The Journal of the Acoustical Society of America, Vol. 53, No. 3, 1973, pp. 771-776.
7. Chou, P.C., and Koenig, H.A., "A Unified Approach to Cylindrical and Spherical Elastic Waves by Method of Characteristics," ASME Journal of Applied Mechanics, Vol. 33, 1966, pp. 159-167.
8. Pao, Y.H., and Ceranoğlu, A.N., "Determination of Transient Responses of a Thick-Walled Spherical Shell by the Ray Theory," ASME Journal of Applied Mechanics, Vol. 45, 1978, pp. 114-122.
9. Born, M., and Wolf, E., Principles of Optics, Pergamon Press, 1975.
10. Van der Pol, B. and Bremmer, H., "The Propagation of Radio Waves Over a Finitely Conducting Spherical Earth," Philosophical Magazine, Vol. 25, 1938, p. 817.
11. Pao, Y.H., and Gajewski, R., "The Generalized Ray-Theory and Transient Elastic Waves in Layered Media," Physical Acoustics, Vol. 13, edited by Mason, W. and Thurston, R., Academic Press, 1977, pp. 183-265.

12. Sechler, E.E., Elasticity in Engineering, John Wiley, 1952.
13. Eringen, A.C., Mechanics of Continua, John Wiley, 1967.
14. Morse, P.M., and Feshbach, H., Methods of Theoretical Physics, McGraw-Hill, New York, 1953, p. 469.
15. Fox, L., An Introduction to Numerical Linear Algebra, Clarendon Press, Oxford, 1964.

REFERENCES NOT CITED

Achenbach, J.D., Wave Propagation in Elastic Solids, North-Holland Publishing Company, 1973.

Kolsky, H., Stress Waves in Solids, Dover Publications, 1963.

Pao, Y.H., and Mow, C.C., Diffraction of Elastic Waves and Dynamic Stress Concentrations, The Rand Corporation, 1973.

Southwell, R.V., An Introduction to the Theory of Elasticity, Oxford University Press, 1941.